Journal of Medicinal Chemistry

Subscriber access provided by - Access paid by the | UCSB Libraries

4-Amino-7,8-dihydro-1,6-naphthyridin-5(6H)-ones as inhaled phosphodiesterase type 4 (PDE4) inhibitors: structural biology and structure-activity relationships (SAR)

Richard S. Roberts, Sara Sevilla, Manel Ferrer, Joan Taltavull, Begoña Hernández, Victor Segarra, Jordi Gracia, Martin D. Lehner, Amadeu Gavaldà, Míriam Andrés, Judit Cabedo, Dolors Vilella, Peter Eichhorn, Elena Calama, Carla Carcasona, and Montserrat Miralpeix

J. Med. Chem., **Just Accepted Manuscript** • DOI: 10.1021/acs.jmedchem.7b01751 • Publication Date (Web): 05 Mar 2018

Downloaded from http://pubs.acs.org on March 5, 2018

Just Accepted

"Just Accepted" manuscripts have been peer-reviewed and accepted for publication. They are posted online prior to technical editing, formatting for publication and author proofing. The American Chemical Society provides "Just Accepted" as a service to the research community to expedite the dissemination of scientific material as soon as possible after acceptance. "Just Accepted" manuscripts appear in full in PDF format accompanied by an HTML abstract. "Just Accepted" manuscripts have been fully peer reviewed, but should not be considered the official version of record. They are citable by the Digital Object Identifier (DOI®). "Just Accepted" is an optional service offered to authors. Therefore, the "Just Accepted" Web site may not include all articles that will be published in the journal. After a manuscript is technically edited and formatted, it will be removed from the "Just Accepted" Web site and published as an ASAP article. Note that technical editing may introduce minor changes to the manuscript text and/or graphics which could affect content, and all legal disclaimers and ethical guidelines that apply to the journal pertain. ACS cannot be held responsible for errors or consequences arising from the use of information contained in these "Just Accepted" manuscripts.

ACS Publications

is published by the American Chemical Society. 1155 Sixteenth Street N.W., Washington, DC 20036

Published by American Chemical Society. Copyright © American Chemical Society. However, no copyright claim is made to original U.S. Government works, or works produced by employees of any Commonwealth realm Crown government in the course of their duties.

4-Amino-7,8-dihydro-1,6-naphthyridin-5(6H)-ones as inhaled phosphodiesterase type 4 (PDE4) inhibitors: structural biology and structure-activity relationships (SAR)

Richard S. Roberts,[§] Sara Sevilla,[§] Manel Ferrer,[§] Joan Taltavull,[#] Begoña Hernández,[§] Victor Segarra,[#] Jordi Gràcia,[#] Martin D. Lehner,[≠] Amadeu Gavaldà,[∂] Miriam Andrés,[#] Judit Cabedo,[#] Dolors Vilella,[§] Peter Eichhorn,[∏] Elena Calama,[∂] Carla Carcasona,[∂] Montserrat Miralpeix[§]*

[#] Almirall S.A., Centro de Investigación y Desarrollo, Medicinal Chemistry & Screening, Crta. Laureà Miró 408-410, Sant Feliu de Llobregat, 08980 Barcelona, Spain.

[∏] Almirall S.A., Centro de Investigación y Desarrollo, Pharmacokinetics & Metabolism, Crta. Laureà Miró 408-410, Sant Feliu de Llobregat, 08980 Barcelona, Spain.

[∂] Almirall S.A., Centro de Investigación y Desarrollo, Experimental Dermatology, Crta. Laureà Miró 408-410, Sant Feliu de Llobregat, 08980 Barcelona, Spain.

[≠] Bionorica SE, Kerschensteinerstraße 11-15, 92318 Neumarkt, Germany.

[§] Former employee of Almirall S.A.

ABSTRACT

Rational design of a novel template of naphthyridinones rapidly led to PDE4 inhibitors with sub-nanomolar enzymatic potencies. X-ray crystallography confirmed the binding mode of this novel template. We achieved compounds with double-digit picomolar enzymatic potencies through further structure-based design by targeting both the PDE4 enzyme metal-binding pocket and occupying the solvent-filled pocket. A strategy for lung retention and long duration of action based on low aqueous solubility was followed. *In vivo* efficacies were measured in a rat lung neutrophilia model by suspension microspray and dry powder administration. Suspension microspray of potent compounds showed *in vivo* efficacy with a clear dose-response. Despite sustained lung levels, dry powder administration performed much less well and without proper dose-response, highlighting clear differences between the two formulations. This indicates a deficiency in the low aqueous solubility strategy for long duration lung efficacy.

INTRODUCTION

Cyclic nucleotide adenosine monophosphate (cAMP) is a ubiquitous secondary messenger involved in a range of cellular responses to biological agents brought about through activation of adenylyl cyclase. Intracellular levels of cAMP are tightly controlled by a family of cyclic nucleotide degrading enzymes, the phosphodiesterases (PDEs). The PDEs are therefore implicated in the control of many biological processes.[1,2,3,4] We were particularly interested in the inflammatory responses modulated by PDE4, especially with respect to chronic obstructive pulmonary disease (COPD). Research into PDE4 inhibitors is decades old, and the recent successful launches of the inhibitors roflumilast (Daliresp **1**) for the oral treatment of COPD and

apremilast (Otezla **2**) for the oral treatment of psoriasis have been long-awaited in the field (Figure 1). PDE4 is therefore still an active target for research and several reviews on the development of PDE4 inhibitor clinical candidates are available.[5,6,7,8,9]

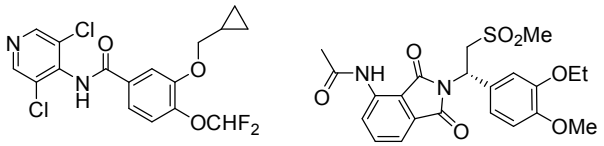

1 roflumilast
oral for COPD
PDE4B1 IC_{50} 0.7 nM

2 apremilast
oral for plaque psoriasis
PDE4B2 IC_{50} 30 nM

Figure 1. Structures and affinities[10] of approved oral drugs roflumilast **1** and apremilast **2**.

Despite these successes, cardiac and emetic side effects are prevalent. PDE4 has four isotypes, PDE4A-D. PDE4B is linked to the anti-inflammatory effects,[11] while the side effects are attributed to PDE4D.[12,13] X-ray crystallography has facilitated the understanding of the catalytic domains of PDE4A-D.[14,15,16] It has also revealed that the four isoforms show little difference in their active sites, and as a result few isoform-selective compounds exist.[17,18] Therefore, to minimize the potential systemic side effects of PDE4, and with special relevant to respiratory diseases, we and many others have turned to inhaled delivery to the lung.[19]

The molecular design of compounds for inhaled delivery has advanced significantly over the last few years.[20] The lung is a highly perfused organ and so highly soluble and permeable compounds - properties which desirable for oral administration - are readily absorbed systemically and therefore of little use as compounds to target the lungs. Inhaled compounds need to stay localized in the lungs and respiratory tract, and so strategies of reduced aqueous solubility and/or increased tissue binding are common.[21,22,23] Reducing systemic exposure through high clearance can help improve the safety profile of compounds: “soft-drugs”

incorporate metabolically-labile groups, susceptible to either plasma hydrolysis or hepatic oxidative phase I or conjugative phase II metabolism.[24] A further approach is to incorporate slow binding kinetics and to dissociate the pharmacodynamics (PD) effect from the pharmacokinetic (PK) profile.[25,26,27] Finally, since the dose of compound that can be administered to the lung is limited, often to a milligram or less in humans,[28] compounds should be as potent as possible. Molecular properties addressing these issues can, and probably should therefore, deviate from properties that are desirable for oral compounds. Since PDE4 is an intracellular target, molecular properties should still be controlled to some degree as cellular permeability is necessary for efficacy and whole-cell assays should be employed to detect any such deficiencies in permeation and target access.

RESULTS AND DISCUSSION

Design of the inhibitors. Here we describe our efforts to discover novel, highly potent (sub-nanomolar), inhaled inhibitors of PDE4 for the treatment of COPD. We were drawn to the series of quinolines from GSK, which showed extremely high potency and had physicochemical properties aligned with inhaled delivery. Quinoline **3** (GSK256066) reached phase II clinical trials for the inhaled treatment of respiratory disorders.[29] In addition, the crystal structure of **3** bound to the catalytic site of PDE4B2B has been published (pdb code: 3gwt).[30] From our own extensive oral PDE4 program we also had obtained crystal structure data for a series of pyridazinone compounds such as **4** (bound to PDE4D, pdb code: 5k1i, Figure 2).[31]

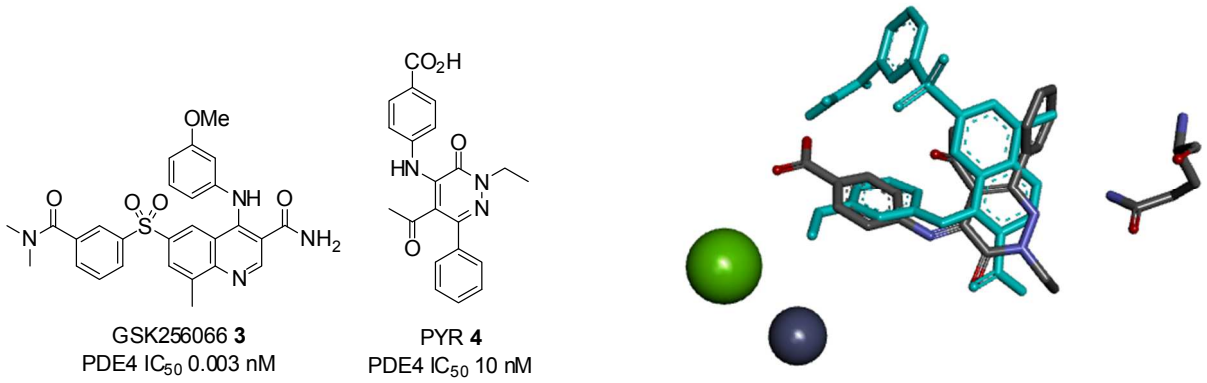

Figure 2. Overlay of the X-ray structures of **4** (colored by element, pdb code: 5kli) and inhaled clinical candidates GSK256066 **3** (in blue, pdb code: 3gwt). Only glutamine-369 and the two metal ions (magnesium in green, zinc in grey) of the PDE4D enzyme are shown.

So, once we overlaid the crystal structure of **4** with that published for the quinoline **3** we could design a new chemical family, the naphthyridinones (NAPs) **5**. We envisaged rapid entry to a new series, taking advantage of the precedent for inhaled delivery of **3** and the known SAR from both families but in an unexploited chemical space with fast synthetic access to compounds with a wide spread of physicochemical properties as desired (Figure 3).

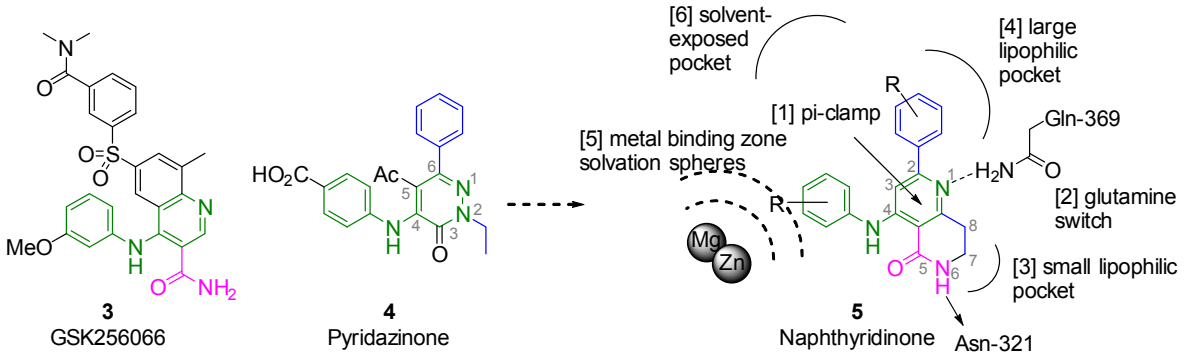

Figure 3. Conceptual design and interactions of the naphthyridinone (NAP) series. Active site regions are defined as follows with respect to the cartoon view above: [1] The pi-clamp region (between Phe-372 and Phe-340). [2] The "glutamine switch" - glutamine-369.[32] [3] The small

lipophilic pocket. [4] The large lipophilic pocket [5]. The metal binding zone containing the zinc and magnesium ions responsible for the catalytic activity. [6] The solvent exposed pocket - in the full PDE4 isoenzyme, the helices of the upstream conserved region (UCR2), a negative regulator of cAMP hydrolysis, partially fill this area.[33] In truncated protein sequences, coding only for the PDE4 active site, this zone is exposed to the bulk solvent, hence the name.

In our design, the aryl-amino-heteroaryl motif (Figure 3, in green) was conserved across the three families. The rigid core of the NAPs would slot into the pi-clamp region [1] with the 4-aminopyridine motif acting as a powerful H-bond acceptor for the glutamine switch [2]. The lactam portion of the NAP would both fill the small lipophilic pocket [3] and be a H-bond donor to interact with Asn-321 in the floor of the active site, as for the quinoline **3**. We could also take advantage of our own internal SAR of the pyridazinone series: firstly for the metal binding zone [5] and secondly for the substitution in the NAP 2-position, filling the large lipophilic pocket [4] and allowing access to the solvent-filled pocket [6]

Syntheis of the Inhibitors. The synthesis of the NAPs has been described previously, as outlined in Scheme 1.[34] Briefly, beta-amino acids **6** were condensed with Meldrum's acid and the resulting tricarbonyl compounds **7** were thermally cyclized to give Boc-protected piperidinediones **8**. Condensation with carbon disulfide and trapping with methyl iodide gave the ketene dithioacetals **9**. The key sequence of the synthesis was the Michael addition of an acetophenone enolate (**9** → **10**) and subsequent condensation-cyclisation with ammonia to form the core of the NAP **11** and with a functionalized handle to introduce the 4-amino substituent. Yields were at best 50% in this sequence **9** → **11**: the two methylthio groups of **9** were of equal

reactivity, but only displacement of the methylthiol group *cis* to the piperidinedione ketone carbonyl (**9** → **10**) led to correct cyclization and pyridine formation. Nevertheless, the route was sufficiently robust to allow large quantities of sulfides **11** to be synthesized. The sulfides **11** were oxidized to the sulfones **12** to increase the reactivity of the leaving group. Finalization of the synthesis to the desired NAPs **5** could be carried out in one of two ways. In the first case, the sulfones were thermally displaced directly with the appropriate amine or aniline. When the displacement was carried out in refluxing ethanol, the Boc protecting group remained largely intact, so this was removed under acidic conditions with a final treatment with trifluoroacetic acid (TFA) (Scheme 1, f). Alternatively, the Boc group could be removed thermally, under microwave irradiation at 160 ºC (Scheme 1, g). Despite liberating carbon dioxide under sealed tube conditions, the increase in pressure was well within the tolerability of the microwave apparatus. For poorly reactive amines, we moved directly to microwave irradiation to carry out the amide displacement and Boc deprotection in one step (Scheme 1, h). In the second route, Boc deprotection of sulfone **12** and displacement of the sulfone with ammonia gave versatile intermediate **13**, which allowed introduction of a range of R^2-substituents via palladium-catalyzed N-arylations (Scheme 1, i-k). Despite the moderate-to-low yields of the key cyclisation sequence **9** → **11**, the modular synthesis allowed us rapid access to a range of substituents to systematically probe the SAR of each position in turn.

Scheme 1. General Synthetic Route to Naphthyridinones 5

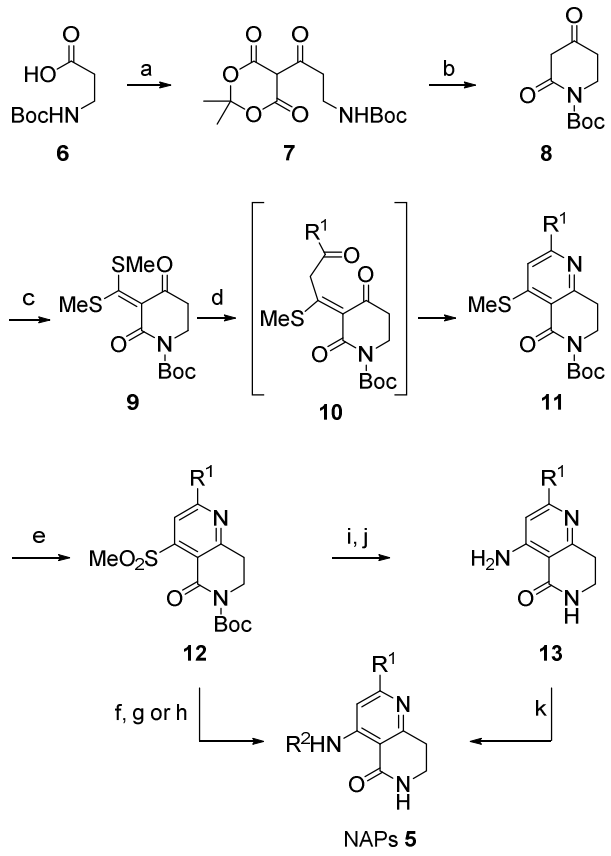

[a] Reagents and Conditions: (a) DCC, DMAP, DCM, 5 ºC, 94% yield; (b) EtOAc, reflux, 83% yield; (c) CS_2, K_2CO_3, DMF, rt then MeI, DMF, 70% yield; (d) R^1COMe, tBuOK, DMSO, THF, rt, 3 h, then NH_4OAc, AcOH, 90 ºC, 6-55% yield; (e) mCPBA, DCM, 5 ºC, 77-100% yield; (f) R^2NH_2, EtOH, reflux, then TFA, DCM, rt if necessary, 20-62% yield; (g) R^2NH_2, EtOH, reflux, then 160 ºC (microwave), 0.5 h, 14-51% yield; (h) R^2NH_2, EtOH, 160 ºC (microwave), 0.5-18 h, 7-83% yield; (i) TFA, DCM, rt; (j) NH_3 (7N in MeOH), 140 ºC (microwave), 67-97% yield over two steps; (k) R^2Hal, Cs_2CO_3, $Pd_2(dba)3$, xantphos, dioxane, 90 ºC, 28-41% yield.

A biaryl substitution pattern in the NAP R^1 position was of particular interest. These compounds **17** were synthesized according to Scheme 2. 3-Bromo-NAPs **14** were simply extended via Suzuki reaction to give biphenyls **17**. Thioethers were also accessible from the

same intermediate **14**. Alternatively, intermediate **15** was first coupled via Suzuki reaction and the resulting amines **16** were N-arylated as before.

Scheme 2. General Synthetic Route to R^3-aryl Substituted Naphthyridinones 17

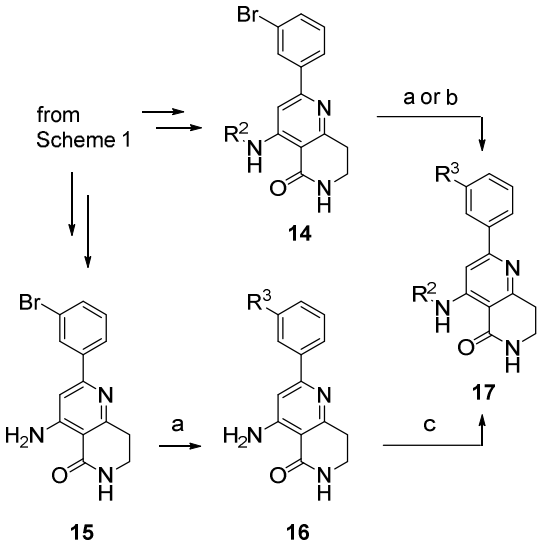

[a] Reagents and Conditions: (a) R^3Hal, Cs_2CO_3, $PdCl_2(dppf)\cdot CH_2Cl_2$, dioxane, 90 ºC, 4-80% yield from **14**, 41-95% yield from **15** (b) thiol, $Pd(PPh_3)_4$, Bu_3SnOMe, xylene, reflux, 64% yield; (c) R^2Hal, $Cs_{1k}O_3$, $Pd_2(dba)3$, xantphos, dioxane, 90 ºC, 9-64% yield.

Deep-reaching NAPs, to study the binding interactions with the floor of the active site, were synthesized as shown in Scheme 3. NAP compounds **5** were converted to their corresponding thiolactams **18** with phosphorous pentasulfide. S-Alkylation with methyl iodide (**19**) and displacement with hydroxylamine or cyanamide gave access to the desired amidoximes and cyanoamidates **20** respectively.

Scheme 3. **General Synthetic Route to Carbonyl-Variant Naphthyridinones 20**

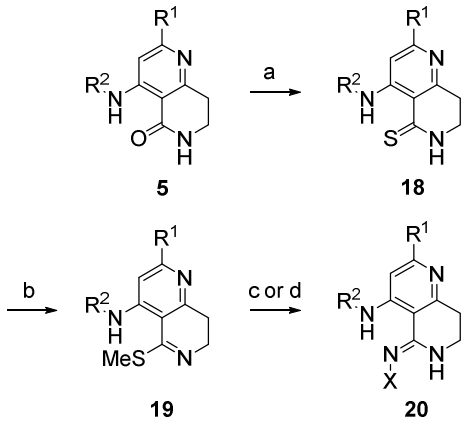

[a] Reagents and Conditions: (a) P_4S_{10}, $iPrNEt_2$, dioxane, 90 ºC, 18 h, 58-99% yield; (b) NaH, MeI, DMF, 60 ºC, 3 h, 81-82% yield; (c) $NH_2OH{\cdot}HCl$, K_2CO_3, EtOH, 70 ºC, 18 h, 23% yield; (d) NH_2CN, EtOH or THF, 70 ºC, 1-2 h, 26-51% yield.

X-ray binding mode of Naphthyridinones. Following the synthetic routes outlined above, the first simple NAP **21** was synthesized and was highly potent with an IC_{50} of 1.6 nM against PDE4B1, corresponding to a high ligand efficiency[35] (LE) of 0.46.

The proposed binding mode of NAP **21**, as outlined in Figure 3, was confirmed by X-ray crystallography (pdb code: 5k32, Figure 4). In addition to the expected interactions, the 3-methoxyaniline substituent was held in place by an intramolecular hydrogen bond between the aniline NH and the lactam carbonyl. The NAP lactam N-H formed a hydrogen bond directly to the side chain of Asn-321 (at 2.7 Å) in the floor of the binding pocket. The lactam also took part in a hydrogen-bonding network with the floor of the binding pocket via a water molecule at 2.5 Å from the lactam carbonyl. In the metal-binding zone, the 3-methoxy group hydrogen bonded (at 3.1 Å) with one of the water molecules in the outer coordination shell of the magnesium ion.

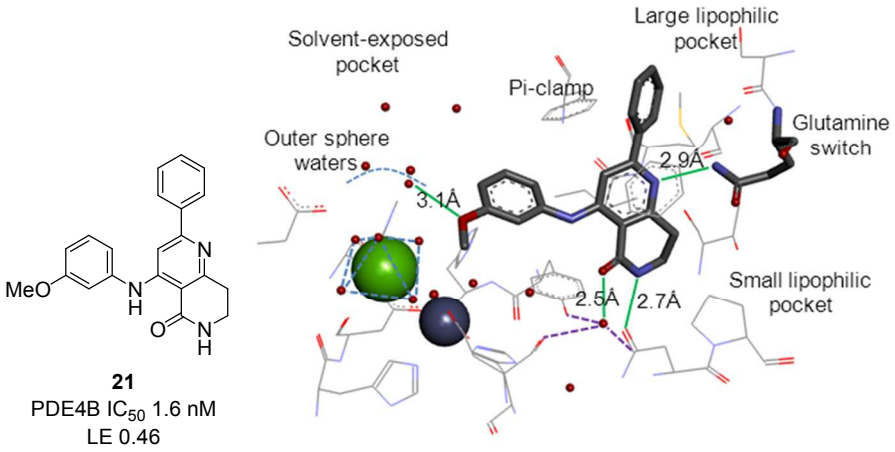

Figure 4. X-ray structure of first synthesized NAP **21** bound to the active site of PDE4D (magnesium, green sphere. zinc, grey. Pdb code: 5k32)

PDE4 inhibitory activity and Structure-Activity Relationships. With the molecular design of the NAPs validated, we expanded the SAR in both the metal binding zone and the large lipophilic / solvent-exposed pocket (Tables 1-7). Compounds were typically tested in two assays. In the first assay, we measured enzyme binding potency through the inhibition of radiolabelled [^{3}H]-cAMP hydrolysis from the human PDE4B1 construct. As PDE4 is an intracellular target, for many compounds we also measured functional inhibition in the production of tumour necrosis factor alpha (TNFα) from peripheral blood mononucleated cell (PBMCs).

We first varied the monocyclic ring in the R^1 position in the large lipophilic pocket with simple substitutions available from acetophenone building blocks (Table 1). In general, little difference was observed in the potency but with two exceptions: the 2-methoxy group (**24**) lost over 10-fold potency, undoubtedly due to a greater twist in the biaryl bond. Pyridyl (**25**) was well-tolerated, however the N-oxide **26** (a synthetic by-product formed during the sulfide to sulfone oxidation step) was not. Clearly, the large lipophilic pocket craves lipophilic groups. Cyclopropyl (**27**) was

also tolerated but other aliphatic R^1 groups were not followed up. Since the R^1 group was introduced from a methyl ketone (see Scheme 1, step (d)), enolization of aliphatic methyl ketones would occur in both directions and mixtures of two regioisomers would occur. Both compounds **21** and **25** displayed similar potencies in the enzymatic assay and the functional cellular assay, indicative of an effective cell permeability. The permeability of compound **21** was measured at 2×10^{-6} cm/s by parallel artificial membrane permeability assay (PAMPA).

Table 1. R^1 Ring Substituent SAR in the Large Lipophilic Pocket

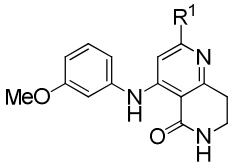

No	R^1	PDE4B IC_{50} (nM)	TNFα IC_{50} (nM)
1	roflumilast	0.70	4.0
21		1.6	5.4
22		8.2	n.d.
23		8.4	n.d.
24		32	n.d.
25		3.6	6.5

26	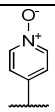	51	n.d.
27		8.5	n.d.

n.d. not determined. All experimental data n≥2. pIC_{50} SD ± <0.2. Data shown to two significant figures.

We also extended the R^1 monocycle to a series of biphenyl groups (Table 2). Here the intention was often two-fold – access the solvent filled pocket with hydrophilic groups and use these groups as metabolic handles for glucuronidation. We derived the meta-substitution pattern from known SAR of our internal PYR series.[31] Biaryl-substituted NAP **28** had a potency of 0.35 nM, further validating our design hypothesis and confirming a close analogy between the PYR and the NAP series.

Biaryl substituted compound, acid **28** was sub-nanomolar in the enzymatic assay. However, this compound showed a 16-fold loss of potency in the cellular assay. Compound **28** showed an acceptable permeability of 3.5×10^{-6} cm/s as measured by the PAMPA assay. Another acid compound, **30** also displayed this loss of potency between the enzymatic and cellular assays. Other factors could be responsible for the loss of activity, for example active transport, not contemplated in the PAMPA assay. This was not investigated further, but we took the shift in potencies as a warning not to proceed with acidic compounds. This shift could be avoided by using the esters **29** and **31** respectively. However, to avoid the complications associated with pharmacologically active prodrugs, we dropped this line of research. A series of amides also gave potent compounds. Amide **34** demonstrated that large groups could be introduced while maintaining enzymatic potency, and could be applicable to the modulation of physical chemical properties at a later date. Cyclopropylamide **33** was particularly effective and showed sub-

nanomolar cellular potency. Phenol (**35**) and thioether (**36**) could also be introduced but with no impact on potency compared to **28**.

Table 2. R^3 Biaryl Substituent SAR Towards the Solvent Exposed Pocket

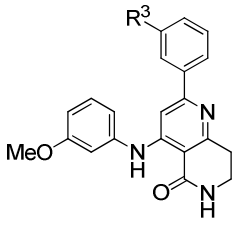

No	R^3	PDE4B IC_{50} (nM)	TNFα IC_{50} (nM)
21	H	1.6	5.4
28	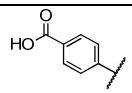	0.35	5.7
29	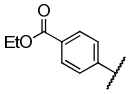	7.2	1.2
30	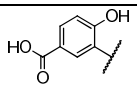	9.6	140
31	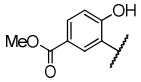	5.6	4.2
32	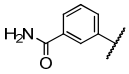	0.28	2.3
33	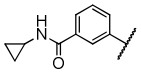	2.1	0.43
34	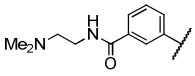	0.23	2.8

35	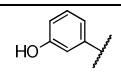	1.8	4.2
36	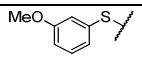	1.6	3.4

All experimental data n≥2. pIC_{50} SD ± <0.2. Data shown to two significant figures.

The X-ray structure of NAP **21** showed the 3-methoxyphenyl R^2 substituent was directed towards the metal binding zone of PDE4, making a hydrogen bond to one of the water molecules in the outer coordination sphere of the magnesium ion. A similar interaction was observed from the benzoic acid group of our pyridazinone **4** (pdb: 5k1i). Many enzymes, particularly the hydrolase family, possess metal ions in their active sites. Metal binding groups, such as thiols, hydroxamic acids or othe bidentate ligands are often used to obtain high affinity inhibitors. However, the common mechanism of metal chelation of these compounds can also lead to a lack of selectivity across this family of enzymes. Through our NAP ligand design, we were not especially troubled by this possibility: firstly, the metal-binding group was designed to target either the outer or inner hydration sphere of the metals, not the metal atoms themselves. Secondly, a large proportion of the binding affinity of our ligands came from the NAP core structure (see zones [1]-[4], Figure 3). Non-selective interactions with other metal-containing enzymes not possessing this specific recognition pattern would therefore be much less potent.

With plenty of opportunity to vary the strength and direction of the hydrogen bonds in that zone, we synthesized a series of analogues. The SAR was reasonably flat (Table 3), with no significant increase of affinity over **21**. An aromatic ring was at least necessary, as demonstrated by the poor activity of truncated amine **37**. Interestingly, despite the drop in potency this compound still maintained a ligand efficiency (LE) of 0.43, little changed from the LE of 0.46 for **21**. Compound **37** could therefore be considered as an efficient fragment for PDE4 and

validation that the NAP core provided much of the binding energy of the whole compound. For the remainder of the changes, small substituents **38-39**, alcohols **40-42**, acid **43**, amides **44-45** and pyridines **46-48** in general showed potencies within an order of magnitude of the first NAP **21**.

Table 3. R^2 Monocyclic Amine SAR in the Metal Binding Zone

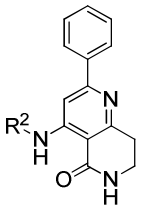

No	R^2	PDE4B IC_{50} (nM)	TNFα IC_{50} (nM)
21	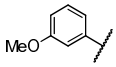	1.6	5.4
37	H	2400	n.d.
38	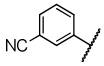	3.3	13
39	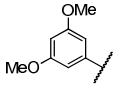	27	n.d.
40	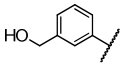	24	n.d.
41	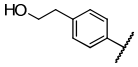	12	n.d.
42	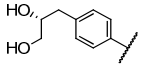	8.7	0.49
43	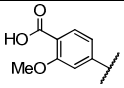	2.3	9.9

44	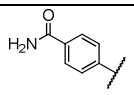	1.5	4.2
45	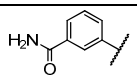	12	n.d.
46		42	n.d.
47	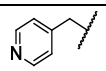	25	n.d.
48	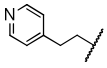	12	n.d.

n.d. not determined. All experimental data n≥2. pIC_{50} SD ± <0.2. Data shown to two significant figures.

We also synthesized bicyclic metal binding groups (Table 4). Plain naphthyl (**49**) lost potency, showing that at least some kind of polar substituent was beneficial. The series of quinoline analogues **50**-**52** showed that the location of this polarity did have some impact. Quinoline **50** was the first compound with sub-nanomolar potency both the enzymatic and the cellular assay. Pyrazolopyridines **53**-**55**, designed to maintain the same interaction as the quinoline **50**, lost potency. Finally, quinoline N-oxide **56** provided a final small increase of potency in both enzymatic and cellular assays. Ligand efficiency of **56** was still high at 0.44.

Table 4. R^2 Bicyclic Amine SAR in the Metal Binding Zone

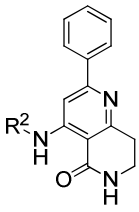

No	R^2	PDE4B IC_{50} (nM)	TNFα IC_{50} (nM)
21	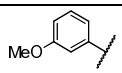	1.6	5.4
49		11	n.d.
50		0.96	0.92
51	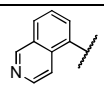	14	n.d.
52	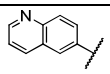	2.3	4.8
53	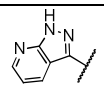	5.6	3.0
54	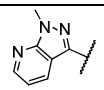	11	n.d.
55	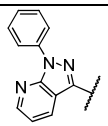	56	n.d.
56	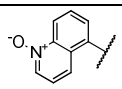	0.43	0.47

n.d. not determined. All experimental data n≥2. pIC_{50} SD ± <0.2. Data shown to two significant figures.

Two other areas were briefly explored: the 3-position of the NAP core and the small lipophilic pocket (Table 5). Pyrimidine analogue **57** was synthesized in a variation of Scheme 1, replacing the acetophenone enolate of step (d) with phenylamidine. Nitrogen at the 3-position of the NAP

core lost potency, possibly because of the weaker hydrogen bonding potential of a 4-aminopyrimidine versus a 4-aminopyridine. Similar structures have been reported with potencies also generally in the double-digit nM range.[36] In the small lipophilic pocket, the role of the C7-C8 ethylene unit of the NAP core was identified. 7-Methyl (**58**) and 8-methyl (**59**) analogues of **21** were synthesized from the appropriate beta-amino acids according to Scheme 1 (in 4% and 15% overall yield respectively). Methyl substitution of these positions resulted in a 70- and 400-fold drop in potency respectively, indicating a close fit to the small lipophilic pocket in the initial design. The lipophilic nature of the ethylene unit to fill the small lipophilic pocket was also evident: open amide structures **60** and **61** lost between 30 and 150-fold potency with respect to their NAP counterparts (**60** ↔ **21** and **61** ↔ **50** respectively).[37] The methyl amide **62** essentially lost all potency - the favored conformation of the amide would direct the methyl group into the floor of the binding site, thus dislodging the rest of the structure from its ideal fitting position. Hence, the initial NAP core design was optimal.

Table 5. Core Variations

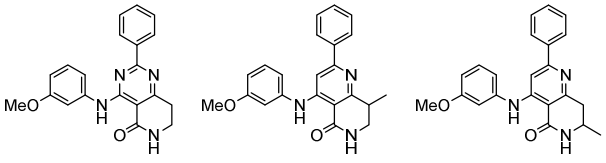

57 **58** **59**

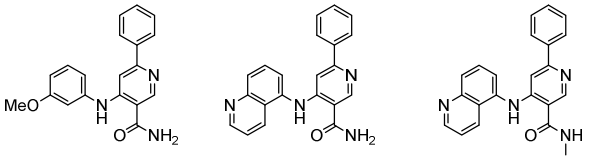

60 **61** **62**

No	PDE4B IC_{50} (nM)	TNFα IC_{50} (nM)

21	1.6	5.4
57	52	40
58	120	270
59	640	n.d.
60	240	n.d.
61	35	n.d.
62	5800	n.d.

n.d. not determined. All experimental data n≥2. pIC_{50} SD ± <0.2. Data shown to two significant figures.

We also extended the NAP lactam group down to the floor of the PDE4 binding site. Displacement of energetically unfavoured water molecules from binding sites can add significant binging affinity, although our approach was done empirically, without applying any of the sophisticated methods for analyzing water molecules.[38] The X-ray crystal structure of NAP **21** showed just a single water molecule between the NAP and the wall of the large lipophilic region, indicating an already close fit (Figure 4). However this water molecule forms a stable H-bonded network between an NH of Gln-369 and the backbone carbonyl of Val-365. We instead targeted the water molecule located at 2.5 Å from the NAP carbonyl (Figure 4). Our approach was to extend the structure down from the NAP carbonyl to leave a polar atom where the water molecule should be.

Some example lactam-containing NAPs were converted to their extended analogues following the steps of Scheme 3 (**24** → **63** and **64**, **65** → **66**, respectively). NAP Hydroxyamidine **63** (N-O bond length typically 1.3 Å) was, as expected, a bond too short, and whether by a steric clash

with the trapped water molecule, or by leaving a high-energy gap between its hydroxyl group and Asn-321, lost three orders of magnitude of potency with respect to the parent NAP **24.** The NAP cyanoamidines **64** and **66** were much more promising (N-C≡N typically 2.5 Å long). While they effectively maintained the enzymatic potency of their NAP lactam analogues, **66** showed some cellular drop-off, so these compounds were not explored further (Table 6).

Table 6. Carbonyl-Variant NAPs to Displace a Deep Water Molecule

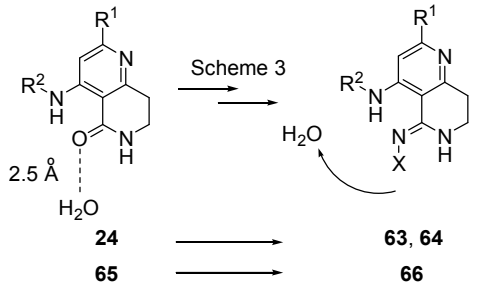

No	R^1	R^2	X	PDE4B IC_{50} (nM)	TNFα IC_{50} (nM)
24		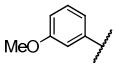	-	8.3	n.d.
63		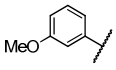	OH	2000	n.d.
64		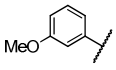	CN	13	n.d.
65	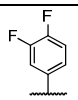		-	0.75	1.5
66	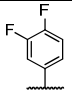		CN	0.89	17

n.d. not determined. All experimental data n≥2. pIC_{50} SD ± <0.2. Data shown to two significant figures.

Finally, some of the best groups of the R^2 and R^3 substituents were combined and the SAR was suitably additive (Table 7). Many of the compounds showed sub-nanomolar potencies in both enzymatic and cellular assays. Of particular interest, quinoline **72** and its N-oxide **73** combined the best R^2 and R^3 substituents from Tables 2 and 4. Quinoline **72** was 170 pM in enzymatic and 120 pM in the cellular assay. N-Oxide **73** was the most potent compound of the series with IC_{50} 45 pM in the enzymatic and 75 pM in the cellular assay. This in vitro activity is comparable to the best compounds of our previous PYR series,[26] from which the selection of the R^2 and R^3 groups of the NAPs were derived.

Table 7. SAR with Combinations of R^2 and R^3.

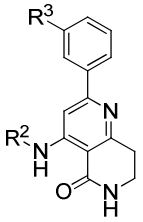

No	R^2	R^3	PDE4B IC_{50} (nM)	TNFα IC_{50} (nM)
21	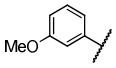	MeO	1.6	5.4
67		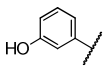	0.89	0.50
68		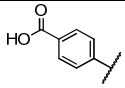	0.11	0.52
69		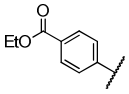	1.2	0.66

70	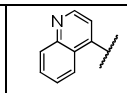	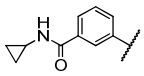	0.27	0.46
71		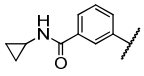	0.32	1.1
72	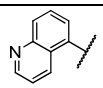	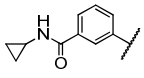	0.17	0.12
73	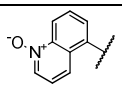	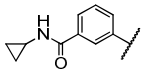	0.045	0.075
74		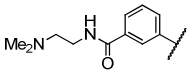	0.11	0.36

All experimental data n≥2. pIC_{50} SD ± <0.2. Data shown to two significant figures.

Lung PK and *In vivo* Neutrophilia in Rats. From the series of NAPs, compound **72** was selected for further profiling, both *in vitro* and *in vivo*, due to its excellent cellular potency in the TNFα assay and to allow like-for-like comparison with other in-house compounds from the PYR series (unpublished results). Permeability of **72** was modest (PAMPA P_{app} 0.15 $\times 10^{-6}$ cm/s). Following our strategy for low aqueous solubility, thermodynamic solubility for **72** was low (4 µg/mL at 37 ºC), but comparable to GSK compound **3** (19 µg/mL at 37 ºC) and higher than that published for roflumilast (0.52 µg/mL at 22ºC).[39] Compound **72** was selective against several other phosphodiesterases and in a counter-screen of 30 kinases (see Supporting Information Table S2). Pharmacokinetic data is shown in Figure 5. Intravenous rat PK at 500 µg/kg showed a moderate-to-high volume of distribution (3.9 L/kg) and a desirably high systemic clearance of around hepatic blood flow (79 mL/min/kg). Intra-tracheal PK in rats using dry powder at 1000 µg/kg (5% w/w with lactose) showed a prolonged exposure. The percentage of the total administered dose present in the lungs reached a maximum of 36% and dropped to 15% over a

24 h period, based on compound recovered from lung biopsies. Corresponding plasma levels measured after intra-tracheal dosing were around or below the level of quantification (<5 ng/mL) up to 1 h post-dose, and undetectable after that (Figure 5).

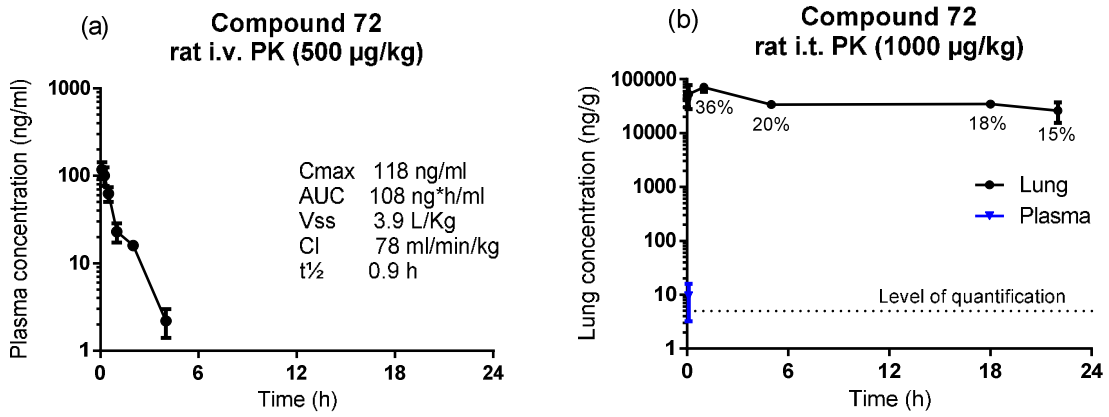

Figure 5. PK profiles of compound **72** in rat. (a) i.v. dose: 500 µg/kg. (b) i.t. dose of dry powder: 1000 µg/kg, as a 5% w/w mixture with lactose. Percentages in the i.t. PK graph refer to the percentage of the total dose (250 µg compound / animal) recovered from the lungs by methanol extraction.

Compound **72** was tested in a rat lipopolysaccharide (LPS)-induced neutrophilia model, measuring the inhibition of increase of neutrophils in the bronchoalveolar lavage (BAL) fluid. Compounds were prepared in aqueous suspension and administered intra-tracheally by micro-spray using the Penn-Century device. Animals were challenged 1 h later with nebulized LPS, with the neutrophilia readout 4 h later, i.e. a total of 5 h after test compound administration. Roflumilast **1** was used as a control, showing a clear dose-response and reaching 80% inhibition at 1000 µg/kg. Compound **72** also showed a clear dose-response, however it only reached an

inhibition of 58% at 1000 μg/kg (Figure 6a). Other compounds were also tested at single doses but showed lower efficacies than **72** (see Supporting information Table S3).

Clinical delivery of inhaled compounds is almost always carried out using a dry powder formulation of active ingredient mixed with a lactose carrier. We also measured inhibition of lung neutrophilia after dry powder i.t. administration of compound **72** with roflumilast **1** as control (Figure 6b). Both compounds were micronized before co-mixing with lactose to enhance their kinetic solubility and lung deposition. Compounds were administered with a dry powder insufflator. Animals were again challenged with nebulized LPS 1 h or 18 h later, with the neutrophilia readout 4 h later, i.e. a total of 5 h or 22 h after test compound administration. Roflumilast again performed well 5 h after dosing, with the inhibition dropping off 22 h post administration. Compound **72** showed much more erratic results: a moderate but sustained efficacy at 100 μg/kg, moderate efficacy but short duration at 1000 μg/kg and a slight improvement of efficacy at 3000 μg/kg at the only tested time of 22 h post-dose. Despite extended lung levels of compound **72**, a maximum of 35% inhibition was seen across this range of doses. The absence of clear dose-responses, either for different doses or at different time-points shows that other factors are impeding the efficacy of **72** in the dry powder formulation.

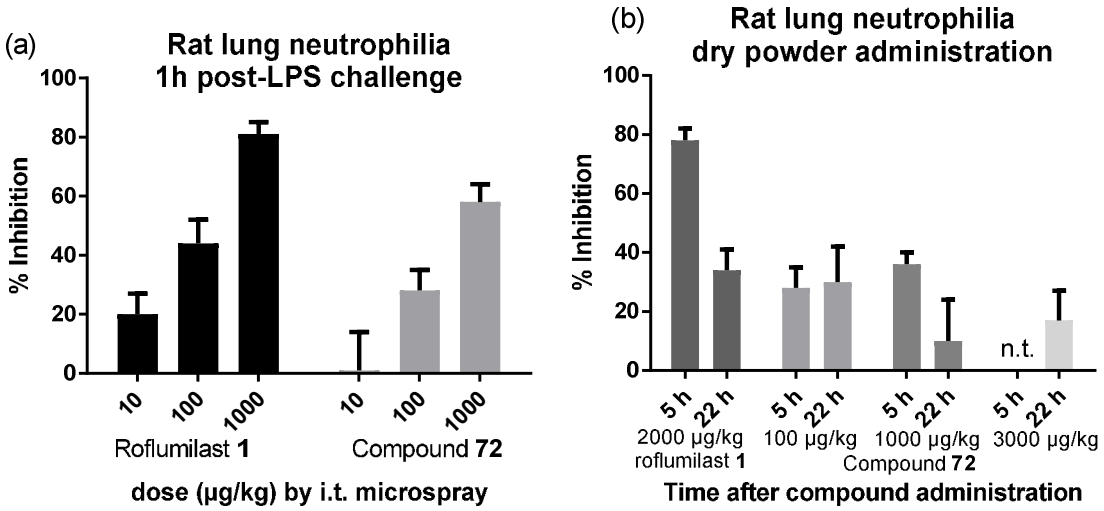

Figure 6. (a) Dose-responses of roflumilast **1** and compound **72** in a LPS-induced rat neutrophilia model. Compounds were administered in suspension by intra-tracheal micro-spray delivery. (b) Time-course inhibition of LPS-induced rat neutrophilia. Roflumilast **1** and compound **72** were given by i.t. administration of dry powder co-mixed with lactose. n.t.: not tested.

The low lung neutrophilia efficacy of compound **72** after inhaled delivery is probably related to its solubility (thermodynamic solubility 4 µg/mL at 37 ºC). Compound **72** was micronized from its amorphous solid/crystalline state without detailed crystallization experiments, and so should represent a more soluble solid form. The separation between lung and plasma levels after i.t. administration is evident of dissolution rate-driven PK (Figure 5b). Despite the apparently long lung PK profile, the lung levels observed were possibly misleading in that they represent the total amount of compound in the lung. A low solubility may well mean that most of the compound remained un-dissolved in solid microparticles, or even phagocytosed by macrophages within the lung, and with little of the total compound dissolved and available to inhibit the PDE4 enzymes present. Lung free fraction or ex-vivo target engagement studies could have shed more light on this situation.

Non-dissolving particles in the lung can often lead to irritation and a pro-inflammatory response. Compound **72** itself was not pro-inflammatory – dry powder administration of 1000 or 3000 μg/kg to the lung did not result in an increase in neutrophils in BAL (0.7-fold and 1.3-fold increase on basal levels observed respectively, n = 4). However, the sustained PK profile of Figure 5b is not characteristic of an effective dissolution in the lung.

Ultimately, in a preliminary safety assay, compound **72** also produced emesis in ferrets in a dose-dependent manner (Table 8).

Table 8. Emetic Events Observed in Ferrets for Compound 72.

Dose (μg/kg)	Emesis observed[a]
30	0 / 4
100	1 / 4
300	3 / 4

[a] number of animals with emesis / number of animals in study. Compound **72** was administered inter-tracheally to ferrets as a dry-powder co-mixture with lactose. Observation lasted 1 h. The first emetic event in each group occurred within 20 min.

CONCLUSIONS

We used rational design based on X-ray crystallography to conceive a novel chemical series of PDE4 inhibitors, the naphthyridoinones (NAPs). The first synthesized example **21** was highly potent at 1.6 nM. A modular chemical synthesis allowed rapid SAR expansion of all substitution positions around the central core. Several examples with sub-nanomolar potencies both in enzymatic assays and inhibition of TNF-α production in whole cells were found. Compound **72** was advanced to the *in vivo* LPS-induced lung neutrophilia in rats. This compound demonstrated

a moderate efficacy, however physicochemical properties seemed to restrict its full potential, especially when dosed as a dry powder formulation. In our other PDE4 series, the pyridazinones,[31] we observed superior *in vivo* results for more soluble compounds, incorporating basic groups to facilitate a long lung duration. We conclude that the low solubility strategy of the NAPs was not ideal: *in vivo* efficacy was compromised for highly potent *in vitro* molecules and erratic kinetic solubility rates can lead to unpredictable or un-reproducible results. The NAP series was abandoned at this stage.

Experimental section

General Chemistry Methods. Reaction products were purified, when necessary, by flash chromatography on silica gel (40-63 μm) with the solvent system indicated. Purifications in reverse phase were made in a Biotage SP1 automated purification system equipped with a C18 column and using a gradient of, unless otherwise stated, water-acetonitrile/MeOH (1:1) (0.1% v/v ammonium formate both phases) from 0% to 100% acetonitrile/MeOH (1:1) in 80 column volumes. Preparative HPLC-MS were performed on a Waters instrument equipped with a 2767 injector/collector, a 2525 binary gradient pump, a 2996 PDA detector, a 515 pump as a make-up pump and a ZQ4000 Mass spectrometer detector. All test compounds were purified to >95% purity by HPLC UV trace unless otherwise stated.

^{1}H Nuclear Magnetic Resonance Spectra were recorded on a Gemini 200 MHz spectrometer or a Varian Mercury plus operating at a frequency of 400 MHz. Tetramethylsilane was used as reference. Chemical shifts (δ) are given in ppm to 2 decimal places. Coupling constants (*J* values) are given in ppm to 1 decimal place. The following abbreviations are used: singlet (s), doublet (d), triplet (t), quartet (q), quintet (quin), double doublet (dd), double triplet (dt), triple

doublet (td), multiplet (m), broad signal (br. s), apparent (app). Partial refers to spectra where a peak or peaks are obscured under solvent peaks and cannot be assigned. Signals of protons attached to heteroatoms may or may not be present according to solvent conditions. Mass Spectra (m/z) were recorded on a Micromass ZMD or in a Waters ZQ mass spectrometer using ESI ionization.

***tert*-Butyl [3-(2,2-dimethyl-4,6-dioxo-1,3-dioxan-5-yl)-3-oxopropyl]carbamate (7).** Boc-beta alanine (**6**) (83 g, 0.44 mol) was dissolved in 2.7 L dichloromethane, which had been previously cooled to 5 ºC in the fridge. Meldrum's acid (66.6 g, 0.46 mol) was added and the mixture shaken to dissolve. 4,4-Dimethylaminopyridine (75 g, 0.61 mol) was added and shaken to dissolve. The solution was left in the fridge for 1 h to cool to approx 5 ºC. Dicyclohexylcarbodiimide (100 g, 0.48 mol) was added, the mixture shaken to dissolve and then left to stand in the fridge (5 ºC) for 2 d. The mixture was filtered and the solid washed twice with cold dichloromethane. The combined filtrates were evaporated to approx 700 mL volume. The organics were washed three times with 10% w/v potassium hydrogen sulfate solution, once with brine and were dried over sodium sulfate. Filtration, evaporation of the filtrate and re-evaporation from ether gave **7** as a white solid (136 g, 0.41 mol, 94% yield), HPLC purity 99%. ^{1}H NMR (200 MHz, $CDCl_3$) δ 1.43 (s, 9H), 1.75 (s, 6H), 3.30 (t, J = 6.4 Hz, 2H), 3.55 (q, J = 5.9 Hz, 2H), 4.85 (br. s., 1H); MS(ESI) m/z 316 $[M + H]^+$.

***tert*-Butyl 2,4-dioxopiperidine-1-carboxylate (8)**. A suspension of **7** (136 g, 0.41 mol) in 250 mL ethyl acetate and heated at reflux (bath temperature 120 ºC) for 2.5 h. The mixture was allowed to cool and was filtered. The filtrate was evaporated, giving an orange semisolid residue. The residue was dissolved in 200 mL diisopropyl ether. The volume of solvent was then

reduced to around 40 mL, precipitating a yellow solid. The solid was collected by filtration, washed twice with diisopropyl ether and dried in a stream of air to give **8** as a pale yellow solid (6.4 g, 30.0 mmol, 62% yield), HPLC purity 100%. ^{1}H NMR (200 MHz, $CDCl_3$) δ 1.56 (s, 9H), 2.63 (t, J = 6.1 Hz, 2H), 3.52 (s, 2H), 4.11 (t, J = 5.9 Hz, 2H); MS(ESI) m/z 212 $[M - H]^-$.

***tert*-Butyl 3-[bis(methylthio)methylene]-2,4-dioxopiperidine-1-carboxylate (9).** A mixture of **8** (22.7 g, 106 mmol) and carbon disulfide (14.0 mL, 232 mmol) were dissolved in 180 mL dry dimethylformamide. Potassium carbonate (31 g, 224 mmol, previously powdered in a mortar) was added and the mixture stirred for 2 h at room temperature, rapidly turning a deep red colour. Methyl iodide (14.0 mL, 225 mmol) dissolved in 50 mL dry dimethylformamide was added to the mixture drop-wise and with stirring over 1 h. cooling the solution during addition using a water bath. Upon addition the mixture was stirred for a further 1 h at room temperature. 400 mL Water and 200 mL 4% w/v sodium carbonate solution were added and the mixture was extracted four times with ether. The combined bright red ether layer was washed with 5% w/v sodium thiosulfate solution, brine and then dried over sodium sulfate. Evaporation of the mixture gave a residue which solidified. The solid was broken up in a little diisopropyl ether and was collected by filtration. The solid was washed with a little diisopropyl ether and was dried in a stream of air to give **9** as a pale yellow solid (21.2 g, 67 mmol, 63% yield), HPLC purity 99%. ^{1}H NMR (200 MHz, $CDCl_3$) δ 1.54 (s, 9H), 2.53 (s, 6H), 2.60 (t, J = 6.1 Hz, 2H), 3.90 (t, J = 6.1 Hz, 2H); MS(ESI) m/z 318 $[M + H]^+$.

***tert*-Butyl 4-(methylthio)-5-oxo-2-phenyl-7,8-dihydro-1,6-naphthyridine-6(5*H*)-carboxylate (11)** (R^1 = Ph). Typical procedure for Michael addition of acetophenone / ammonia condensation sequence (Scheme 1, conditions d). **Method 1d.** A mixture of **9** (9.95 g, 31.3

mmol) and acetophenone (7.6 g, 63.3 mmol) were dissolved in 250 mL dimethylsulfoxide and 200 mL tetrahydrofuran. Potassium tert-butoxide (10.5 g, 93.6 mmol) was added in three equal portions at 30 min intervals, giving a dark red solution. After addition, the mixture was stirred for 2 h. Ammonium acetate (25 g, 324 mmol) was added followed by 200 mL acetic acid. The solution warmed and paled slightly. The mixture was heated at 90 ºC for 2 h, allowed to cool to room temperature and was diluted with 200 mL water. The mixture was then cooled in an ice-water bath and was carefully neutralized with slow addition of approx 400 mL 8N sodium hydroxide solution. Solid sodium carbonate was then carefully added to basify the solution to pH 11. The mixture was extracted four times with ether. The combined ether layers were washed with brine, dried over sodium sulfate, filtered and evaporated. The residue purified by column chromatography (ethyl acetate-hexane, 20:80) to give **11** (R^1 = Ph) as a pale yellow solid (4.02 g, 10.7 mmol, 37% yield), HPLC purity 98%. ^{1}H NMR (400 MHz, $CDCl_3$) δ 1.60 (s, 9H), 2.51 (s, 3H), 3.23 (t, *J* = 6.3 Hz, 2H), 4.03 (t, *J* = 6.3 Hz, 2H), 7.45 - 7.55 (m, 4H), 8.01 (d, *J* = 6.7 Hz, 2H); MS(ESI) *m*/*z* 371 $[M + H]^+$.

***tert*-Butyl 4-(methylsulfonyl)-5-oxo-2-phenyl-7,8-dihydro-1,6-naphthyridine-6(5*H*)-carboxylate (12)**, R^1 = Ph. Typical procedure for oxidation of sulfide to sulfone (Scheme 1, conditions e). **Method 1e.** A solution of **11** (R^1 = Ph, 4.02 g, 10.8 mmol) dissolved in 150 mL dichloromethane was cooled to 5 ºC in an ice-bath. *meta*-Chloroperbenzoic acid (max purity 77%, 7.25 g, 32.4 mmol) was added and the mixture was stirred for 30 min at 5 ºC. The mixture was then stirred at room temperature for 2 h. The organics were washed three times with 4% w/v sodium carbonate solution, once with brine and dried over sodium sulfate. Filtration and evaporation gave **12** (R^1 = Ph) as a white solid (4.40 g, 10.7 mmol, 99% yield), HPLC purity 99%. ^{1}H NMR (400 MHz, $CDCl_3$) δ 1.60 (s, 9H), 3.33 (t, *J* = 6.1 Hz, 2H), 3.69 (s, 3H), 4.10 (t,

J = 6.1 Hz, 2H), 7.50 - 7.57 (m, 3H), 8.14 (dd, *J* = 6.5, 2.9 Hz, 2H), 8.50 (s, 1H); MS(ESI) *m*/*z* 420 $[M + NH_4]^+$.

4-Amino-2-(3-bromophenyl)-7,8-dihydro-1,6-naphthyridin-5(6*H*)-one (15). Method 1ij (see compound **37**). Tan solid. 88% Yield over 2 steps from **12** (R^1 = 3-BrPh), HPLC purity 96%. ^{1}H NMR (400 MHz, $CDCl_3$) δ 3.12 (t, *J* = 6.8 Hz, 2H), 3.59 (td, *J* = 6.7, 2.5 Hz, 2H), 5.71 (br. s., 2H), 6.79 (s, 1H), 7.31 (t, *J* = 7.8 Hz, 1H), 7.53 (d, *J* = 7.8 Hz, 1H), 7.84 (d, *J* = 7.8 Hz, 1H), 8.11 (s, 1H); MS(ESI) *m*/*z* 318, 320 $[M + H]^+$.

4-[(3-Methoxyphenyl)amino]-2-phenyl-7,8-dihydro-1,6-naphthyridin-5(6*H*)-one (21). Typical procedure for sulfide displacement with amines and anilines under conventional heating and subsequent Boc-deprotection under acidic conditions (Scheme 1, conditions f). **Method 1f.** Step 1. A mixture of **12** (R^1 = Ph, 50 mg, 0.124 mmol) and 3-methoxyaniline (74 mg, 0.60 mmol) was suspended in 1 mL ethanol and agitated at 70 ºC overnight in a capped vial. The mixture was allowed to cool and was was partitioned between saturated sodium carbonate solution and ether. The aqueous was extracted twice with ether and the combined organics were washed with brine and dried over sodium sulfate, filtered and evaporated to give a residue. The residue was purified by column chromatography (ethyl acetate-hexane, 50:50) to give *tert-butyl 4-[(3-methoxyphenyl)amino]-5-oxo-2-phenyl-7,8-dihydro-1,6-naphthyridine-6(5H)-carboxylate.*

Step 2. This compound was dissolved directly in 0.3 mL dichloromethane and 0.5 mL trifluoroacetic acid was added. After 10 min at room temperature, the mixture was reduced in volume in a stream of nitrogen and was partitioned between saturated sodium carbonate solution and ether. The aqueous was extracted twice with ether. The combined organics were washed with brine and dried over sodium sulfate. Filtration and evaporation gave a residue which was

purified by column chromatography (ethyl acetate-hexane, gradient) to give **21** as a pale yellow solid (26 mg, 0.075 mmol, 60% yield), HPLC purity 99%. ^{1}H NMR (400 MHz, $CDCl_3$) δ 3.18 (t, *J* = 6.7 Hz, 2H), 3.64 (td, *J* = 6.7, 2.7 Hz, 2H), 3.82 (s, 3H), 5.80 (br. s., 1H), 6.76 (dd, *J* = 8.2, 2.2 Hz, 1H), 6.84 (s, 1H), 6.92 (d, *J* = 7.8 Hz, 1H), 7.31 (t, *J* = 8.2 Hz, 1H), 7.36 (s, 1H), 7.38 - 7.46 (m, 3H), 7.87 (d, *J* = 7.5 Hz, 2H), 10.77 (s, 1H); MS(ESI) *m*/*z* 346 $[M + H]^+$.

2-(3-Bromophenyl)-4-[(3-methoxyphenyl)amino]-7,8-dihydro-1,6-naphthyridin-5(6*H*)-one (22). Typical procedure for direct sulfide displacement with amines and anilines under microwave heating (Scheme 1, conditions h). **Method 1h.** A mixture of **12** (R^1 = 3-BrPh, 224 mg, 0.47 mmol) and 3-methoxyaniline (0.30 g mg, 2.45 mmol) were suspended in 10 mL ethanol and were heated at 160 ºC (max pressure 12 bar) for 9 h under microwave irradiation. The mixture was allowed to cool and was evaporated under reduced pressure. The residue was taken up in dichloromethane and the organics washed three times with 4% w/v sodium carbonate solution, once with brine and dried over sodium sulfate. Filtration and evaporation gave a residue which was purified by column chromatography (ethyl acetate-hexane, gradient) to give **22** as a white solid (150 mg, 0.35 mmol, 76% yield), HPLC purity 99%. ^{1}H NMR (200 MHz, $CDCl_3$) δ 3.17 (t, *J* = 6.7 Hz, 2H), 3.64 (td, *J* = 6.7, 2.5 Hz, 2H), 3.83 (s, 3H), 5.82 (br. s., 1H), 6.78 (d, *J* = 8.2 Hz, 1H), 6.83 (s, 1H), 6.91 (d, *J* = 8.2 Hz, 1H), 7.21 - 7.39 (m, 3H), 7.52 (d, *J* = 8.2 Hz, 1H), 7.74 (d, *J* = 7.8 Hz, 1H), 8.08 (s, 1H), 10.80 (s, 1H); MS(ESI) *m*/*z* 424,426 $[M + H]^+$.

2-(3-Methoxyphenyl)-4-[(3-methoxyphenyl)amino]-7,8-dihydro-1,6-naphthyridin-5(6*H*)-one (23). Method 1h. Pale brown solid, HPLC purity 98%. 51% Yield from **12** (R^1 = 3-MeOPh) and 3-methoxyaniline. ^{1}H NMR (200 MHz, $CDCl_3$) δ 3.17 (t, *J* = 6.8 Hz, 2H), 3.63 (td, *J* = 6.5,

2.5 Hz, 2H), 3.82 (s, 3H), 3.86 (s, 3H), 6.02 (br. s., 1H), 6.75 (d, *J* = 8.2 Hz, 1H), 6.83 (s, 1H), 6.86 - 6.99 (m, 2H), 7.27 - 7.51 (m, 5H), 10.76 (s, 1H); MS(ESI) *m*/*z* 376 $[M + H]^+$.

2-(2-Methoxyphenyl)-4-[(3-methoxyphenyl)amino]-7,8-dihydro-1,6-naphthyridin-5(6*H*)-one (24). Method 1h. Pale brown solid, HPLC purity 96%. 71% Yield from **12** (R^1 = 2-MeOPh) and 3-methoxyaniline. ^{1}H NMR (200 MHz, $CDCl_3$) δ 3.15 (t, *J* = 6.6 Hz, 2H), 3.61 (td, *J* = 6.6, 2.5 Hz, 2H), 3.81 (s, 3H), 3.84 (s, 3H), 6.07 (br. s., 1H), 6.69 (d, *J* = 7.4 Hz, 1H), 6.83 - 6.98 (m, 3H), 7.03 (t, *J* = 7.4 Hz, 1H), 7.19 - 7.41 (m, 2H), 7.58 (s, 1H), 7.78 (d, *J* = 7.4 Hz, 1H), 10.72 (s, 1H); MS(ESI) *m*/*z* 376 $[M + H]^+$.

4-[(3-Methoxyphenyl)amino]-2-pyridin-4-yl-7,8-dihydro-1,6-naphthyridin-5(6*H*)-one (25) and **4-[(3-Methoxyphenyl)amino]-2-(1-oxidopyridin-4-yl)-7,8-dihydro-1,6-naphthyridin-5(6*H*)-one (26).** Thiol oxidation (scheme 1, step e) of 11 (R^1 = 4-pyr) gave intermediate **12** as a mixture of pyridine and pyridine N-oxide. This mixture was treated using the Method 1h and separated chromatographically at that point. **25**: Off-white solid, HPLC purity 97%. 39% Yield from **12** (R^1 = 4-Pyr/4-Pyr N-oxide mixture) and 3-methoxyaniline. ^{1}H NMR (200 MHz, $CDCl_3$) δ 3.18 (t, *J* = 6.6 Hz, 2H), 3.65 (td, *J* = 6.5, 2.5 Hz, 2H), 3.83 (s, 3H), 5.80 (br. s., 1H), 6.69 - 6.99 (m, 3H), 7.17 - 7.36 (m, 1H), 7.40 (s, 1H), 7.76 (d, *J* = 5.9 Hz, 2H), 8.67 (d, *J* = 5.5 Hz, 2H), 10.83 (br. s., 1H); MS(ESI) *m*/*z* 347 $[M + H]^+$. **26**: Yellow solid, HPLC purity 100%. 9% Yield from **12** (R^1 = 4-Pyr/4-Pyr N-oxide mixture) and 3-methoxyaniline. ^{1}H NMR (200 MHz, $CDCl_3$) δ 3.14 (t, *J* = 6.6 Hz, 2H), 3.64 (td, *J* = 6.6, 2.5, Hz, 2H), 3.83 (s, 3H), 5.92 (br. s., 1H), 6.73 - 6.85 (m, 2H), 6.89 (d, *J* = 8.2 Hz, 1H), 7.28 - 7.42 (m, 2H), 7.84 (d, *J* = 7.0 Hz, 2H), 8.22 (d, *J* = 7.0 Hz, 2H), 10.83 (br. s., 1H); MS(ESI) *m*/*z* 363 $[M + H]^+$.

2-Cyclopropyl-4-[(3-methoxyphenyl)amino]-7,8-dihydro-1,6-naphthyridin-5(6*H*)-one (27). Method 1h. Off-white solid, HPLC purity 97%. 31% yield from **12** (R^1 = cPr) and 3-methoxyaniline: ^{1}H NMR (200 MHz, $CDCl_3$) δ 0.75 - 1.05 (m, 4H), 1.96 - 2.12 (m, 1H), 3.15 (t, *J* = 6.6 Hz, 2H), 3.58 (td, *J* = 6.6, 2.3 Hz, 2H), 3.83 (s, 3H), 5.75 (br. s., 1H), 6.64 (s, 1H), 6.71 - 6.80 (m, 2H), 6.84 (d, *J* = 8.2 Hz, 1H), 7.29 - 7.37 (m, 1H), 10.82 (br. s., 1H); MS(ESI) *m*/*z* 310 $[M + H]^+$.

3'-{4-[(3-Methoxyphenyl)amino]-5-oxo-5,6,7,8-tetrahydro-1,6-naphthyridin-2-yl}biphenyl-4-carboxylic acid (28). Typical procedure for Suzuki reaction (Scheme 2, conditions a). **Method 2a.** A mixture of **22** (80 mg, 0.19 mmol), 4-carboxyphenylboronic acid (47 mg, 0.28 mmol) and 2M cesium carbonate (0.28 mL, 0.57 mmol) were suspended in 2 mL of degassed dioxane in a sealed tube. The mixture was subjected to three cycles of evacuation-backfilling with argon. 1'-Bis(diphenylphosphino)ferrocene-palladium(II) dichloride dichloromethane complex (8 mg, 0.01 mmol) was added and the mixture was subjected again to three cycles of evacuation-backfilling with argon and then heated at 90 ºC for 3 h. The mixture was allowed to cool to room temperature and the solvent was evaporated. The crude was purified by column chromatography using the SP1 Purification system (ethyl acetate-hexane gradient) to give **28** as a beige solid (58 mg, 0.12 mmol, 66% yield), HPLC purity 100%. ^{1}H NMR (200 MHz, DMSO-d_6) δ 3.03 (t, *J* = 6.4 Hz, 2H), 3.51 - 3.67 (m, 2H), 3.79 (s, 3H), 6.77 (dd, *J* = 8.0, 2.0 Hz, 1H), 6.89 - 7.01 (m, 2H), 7.35 (t, *J* = 8.0 Hz, 1H), 7.50 (s, 1H), 7.58 (t, *J* = 7.8 Hz, 1H), 7.67 - 7.83 (m, 3H), 7.89 (d, *J* = 7.8 Hz, 1H), 8.03 (d, *J* = 8.2 Hz, 2H), 8.17-8.28 (m, 2H), 11.13 (s, 1H); MS(ESI) *m*/*z* 466 $[M + H]^+$.

Ethyl 3'-{4-[(3-methoxyphenyl)amino]-5-oxo-5,6,7,8-tetrahydro-1,6-naphthyridin-2-yl}biphenyl-4-carboxylate (29). Method 2a. White solid, HPLC purity 96%. 22% Yield from **22** and 4-(ethoxycarbonyl)phenylboronic acid: ^{1}H NMR (200 MHz, $CDCl_3$) δ 1.42 (t, *J* = 7.0 Hz, 3H), 3.19 (t, *J* = 6.8 Hz, 2H), 3.65 (td, *J* = 6.8, 2.3 Hz, 2H), 3.82 (s, 3H), 4.41 (q, *J* = 7.3 Hz, 2H), 5.77 (br. s., 1H), 6.76 (dd, *J* = 8.6, 2.5 Hz, 1H), 6.85 (s, 1H), 6.92 (d, *J* = 7.8 Hz, 1H), 7.29 - 7.38 (m, 1H), 7.41 (s, 1H), 7.51 (t, *J* = 7.6 Hz, 1H), 7.59 - 7.65 (m, 1H), 7.70 (d, *J* = 8.2 Hz, 2H), 7.83 (d, *J* = 7.8 Hz, 1H), 8.12 (d, *J* = 8.2 Hz, 2H), 8.17 (s, 1H), 10.81 (s, 1H); MS(ESI) *m*/*z* 494 $[M + H]^+$.

6-Hydroxy-3'-{4-[(3-methoxyphenyl)amino]-5-oxo-5,6,7,8-tetrahydro-1,6-naphthyridin-2-yl}biphenyl-3-carboxylic acid (30). Lithium hydroxide (42 mg, 1.00 mmol) was added to a solution of **31** (50 mg, 0.10 mmol) dissolved in a mixture of tetrahydrofuran/water and the mixture was stirred at 40 ºC for 3 days. The solvent was evaporated, water was added and the pH was adjusted to 5. The resulting suspension was filtered, the solid was washed with diethyl ether and dried to give **30** as a tan solid (25 mg, 0.051 mmol, 51% yield), HPLC purity 97%. ^{1}H NMR (400 MHz, DMSO-d_6) δ 3.15 (t, *J* = 6.4 Hz, 2H), 3.61 (td, *J* = 6.6, 2.5 Hz, 2H), 3.78 (s, 3H), 6.87 (br. s., 1H), 6.94 - 7.06 (m, 2H), 7.20 (d, *J* = 8.6 Hz, 1H), 7.25 - 7.35 (m, 1H), 7.40 (t, *J* = 7.6 Hz, 1H), 7.58 (br. s., 1H), 7.67 - 7.76 (m, 1H), 7.76 - 7.83 (m, 2H), 7.89 (br. s., 1H), 8.00 (br. s., 1H), 8.53 (br. s., 1H), 10.87 (br. s., 1H), 11.77 (br. s., 1H); MS(ESI) *m*/*z* 482 $[M + H]^+$.

Methyl 6-hydroxy-3'-{4-[(3-methoxyphenyl)amino]-5-oxo-5,6,7,8-tetrahydro-1,6-naphthyridin-2-yl}biphenyl-3-carboxylate (31). Methyl 3-bromo-4-hydroxybenzoate (1.51 g, 6.53 mmol) was dissolved in 40 mL of previously degassed dioxane. Bis(pinacolate)diboron (3.32 g, 13.1 mmol), (diphenylphosphino)ferrocene (0.18 g, 0.32 mmol) and potassium acetate

(1.92 g, 19. 6 mmol) were added and the mixture was subjected to three cycles of evacuation-backfilling with argon. 1,1'-Bis(diphenylphosphino)ferrocene-palladium(II) dichloride dichloromethane complex (0.27 g, 0.33 mmol) was added and the mixture was subjected again to three cycles of evacuation-backfilling with argon and heated at 80 ºC for 18 h. The mixture was cooled to room temperature, water and ethyl acetate were added, the organic layer was separated and washed with brine. The aqueous layer was extracted twice with ethyl acetate and the combined organic layers were dried with magnesium sulfate, filtered and evaporated. After purification by column chromatography using the SP1 Purification system (ethyl acetate-hexane gradient) *methyl 4-hydroxy-3-(4,4,5,5-tetramethyl-1,3,2-dioxaborolan-2-yl)benzoate* as a white solid (1.07 g, 3.75 mmol, 57% yield): ^{1}H NMR (200 MHz, $CDCl_3$) δ 1.39 (s, 12H), 3.88 (s, 3H), 6.91 (d, *J* = 8.6 Hz, 1H), 8.06 (dd, *J* = 8.6, 2.3 Hz, 1H), 8.23 (s, 1H), 8.33 (d, *J* = 2.3 Hz, 1H); MS(ESI) *m*/*z* 279 $[M + H]^+$. **31**: Method 2a. Tan solid, HPLC purity 98%. 39% Yield from **22** and methyl 4-hydroxy-3-(4,4,5,5-tetramethyl-1,3,2-dioxaborolan-2-yl)benzoate: ^{1}H NMR (200 MHz, DMSO-d_6) δ 3.01 (t, *J* = 6.4 Hz, 2H), 3.47 (td, *J* = 6.6, 2.5 Hz, 2H), 3.77 (s, 3H), 3.81 (s, 3H), 6.76 (d, *J* = 8.6 Hz, 1H), 6.86 - 7.00 (m, 2H), 7.06 (d, *J* = 8.2 Hz, 1H), 7.34 (t, *J* = 8.0 Hz, 1H), 7.45 (s, 1H), 7.51 (t, *J* = 7.8 Hz, 1H), 7.57 - 7.66 (m, 1H), 7.78 - 7.93 (m, 3H), 8.08 (s, 1H), 8.19 (br. s., 1H), 10.58 (br. s., 1H), 11.11 (s, 1H); MS(ESI) *m*/*z* 496 $[M + H]^+$.

3'-{4-[(3-Methoxyphenyl)amino]-5-oxo-5,6,7,8-tetrahydro-1,6-naphthyridin-2-yl}biphenyl-3-carboxamide (32). Method 2a. White solid. 65% Yield from **22** and 3-carbamoylphenylboronic acid: ^{1}H NMR (200 MHz, $CDCl_3$) δ 3.19 (t, *J* = 6.8 Hz, 2H), 3.64 (t, *J* = 6.8 Hz, 2H), 3.82 (s, 3H), 6.77 (dd, *J* = 8.2, 2.5 Hz, 1H), 6.86 (t, *J* = 2.0 Hz, 1H), 6.92 (d, *J* = 7.8 Hz, 1H), 7.35 (d, *J* = 8.5 Hz, 1H), 7.38 (s, 1H), 7.51 (t, *J* = 7.4 Hz, 1H), 7.54 (t, *J* = 7.4 Hz,

1H), 7.61 - 7.72 (m, 2H), 7.79 (t, *J* = 8.0 Hz, 1H), 7.87 (d, *J* = 7.8 Hz, 1H), 8.16 (s, 2H), 10.80 (s, 1H); MS(ESI) *m*/*z* 465 $[M + H]^+$.

***N*-Cyclopropyl-3'-{4-[(3-methoxyphenyl)amino]-5-oxo-5,6,7,8-tetrahydro-1,6-naphthyridin-2-yl}biphenyl-3-carboxamide (33).** Method 2a. Pale yellow solid, HPLC purity 99%. 48% Yield from **22** and 3-(cyclopropylcarbamoyl)phenylboronic acid: ^{1}H NMR (200 MHz, $CDCl_3$) δ 0.58 - 0.70 (m, 2H), 0.89 (td, *J* = 7.0, 6.0 Hz, 2H), 2.86 - 3.01 (m, 1H), 3.19 (t, *J* = 6.6 Hz, 2H), 3.65 (td, *J* = 6.6, 2.3 Hz, 2H), 3.81 (s, 3H), 5.78 (br. s., 1H), 6.31 (br. s., 1H), 6.75 (dd, *J* = 8.0, 2.5 Hz, 1H), 6.85 (t, *J* = 2.0 Hz, 1H), 6.92 (d, *J* = 8.2 Hz, 1H), 7.29 - 7.37 (m, 1H), 7.41 (s, 1H), 7.49 (t, *J* = 7.6 Hz, 2H), 7.57 - 7.67 (m, 1H), 7.67 - 7.85 (m, 3H), 7.98 (s, 1H), 8.15 (s, 1H), 10.81 (s, 1H); MS(ESI) *m*/*z* 505 $[M + H]^+$.

***N*-[2-(Dimethylamino)ethyl]-3'-{4-[(3-methoxyphenyl)amino]-5-oxo-5,6,7,8-tetrahydro-1,6-naphthyridin-2-yl}biphenyl-3-carboxamide (34).** *N*,*N*-Dimethylethane-1,2-diamine (0.71 g, 8.06 mmol) was added to a solution of 3-(4,4,5,5-tetramethyl-1,3,2-dioxaborolan-2-yl)benzoic acid (1.00 g, 4.03 mmol), 1-hydroxybenzotriazole hydrate (0.82 g, 6.05 mmol) and *N*-ethyl-*N*'-(3-dimethylaminopropyl)carbodiimide hydrochloride (1.16 g, 6.05 mmol) in 8 mL dimethylformamide. The mixture was stirred at room temperature for 3 h. The solvent was removed under reduced pressure and the residue taken up in 4% sodium bicarbonate solution. The aqueous phase was extracted three times with ethyl acetate. The combined organic layers were washed with water and brine, and dried over anhydrous sodium sulfate. The solvent was removed under reduced pressure to give *N-[2-(dimethylamino)ethyl]-3-(4,4,5,5-tetramethyl-1,3,2-dioxaborolan-2-yl)benzamide* as a white solid (0.81 g, 2.55 mmol, 63%): MS(ESI) *m*/*z* 319 $[M + H]^+$. **34**: Method 2a. Brown solid, HPLC purity 95%. 80% Yield from **22** and N-[2-

(dimethylamino)ethyl]-3-(4,4,5,5-tetramethyl-1,3,2-dioxaborolan-2-yl)benzamide: ^{1}H NMR (200 MHz, $CDCl_3$) δ 2.50 (s, 6H), 2.88 (t, *J* = 5.3 Hz, 2H), 3.09 (t, *J* = 6.4 Hz, 2H), 3.47 - 3.62 (m, 2H), 3.64 - 3.77 (m, 2H), 3.80 (s, 3H), 6.44 (br. s., 1H), 6.73 (d, *J* = 8.2 Hz, 1H), 6.83 (br. s., 1H), 6.89 (d, *J* = 8.2 Hz, 1H), 7.27 - 7.38 (m, 2H), 7.44 (t, *J* = 8.0 Hz, 1H), 7.48 (t, *J* = 8.2 Hz, 1H), 7.57 - 7.80 (m, 4H), 7.86 (d, *J* = 7.8 Hz, 1H), 8.13 (br. s., 1H), 8.16 (br. s., 1H), 10.71 (s, 1H); MS(ESI) *m*/*z* 536 $[M + H]^+$.

2-(3'-Hydroxybiphenyl-3-yl)-4-[(3-methoxyphenyl)amino]-7,8-dihydro-1,6-naphthyridin-5(6*H*)-one (35). Method 2a. White solid, HPLC purity 99%. 65% Yield from **22** and 3-hydroxyphenylboronic acid: ^{1}H NMR (200 MHz, $CDCl_3$) δ 3.17 (t, *J* = 6.8 Hz, 2H), 3.63 (t, *J* = 6.8 Hz, 2H), 3.83 (s, 3H), 6.78 (dd, *J* = 8.2, 2.0 Hz, 1H), 6.81 - 6.88 (m, 2H), 6.91 (d, *J* = 7.8 Hz, 1H), 7.07 - 7.19 (m, 2H), 7.21 - 7.39 (m, 4H), 7.47 (t, *J* = 7.8 Hz, 1H), 7.58 - 7.71 (m, 2H), 8.06 (s, 1H), 10.79 (s, 1H); MS(ESI) *m*/*z* 438 $[M + H]^+$.

4-[(3-Methoxyphenyl)amino]-2-{3-[(3-methoxyphenyl)thio]phenyl}-7,8-dihydro-1,6-naphthyridin-5(6*H*)-one (36). Compound **22** (120 mg, 0.28 mmol) was dissolved in 2 mL of xylene in a sealed tube. 3-Methoxybenzenethiol (0.071 mL, 0.56 mmol) and tributyltin methoxide (167 mg, 0.56 mmol) were added and the mixture was heated at 140 ºC for 10 min. Tetrakis(triphenylphosphine)palladium (65 mg, 0.06 mmol) was added and the mixture was stirred at 140 ºC overnight. The mixture was cooled to room temperature and the solvent was evaporated. Ethyl acetate was added and the organic phase was washed with water (x3) and brine (x3). The combined aqueous layers were extracted twice with ethyl acetate and the combined organic layers were dried with magnesium sulfate, filtered and evaporated. The crude was purified by chromatography using the SP1 purification system to give **36** as a pale yellow

solid (89 mg, 0.18 mmol, 64% yield), HPLC purity 98%: ^{1}H NMR (200 MHz, $CDCl_3$) δ 3.15 (t, *J* = 6.8 Hz, 2H), 3.63 (td, *J* = 6.7, 2.5 Hz, 2H), 3.74 (s, 3H), 3.81 (s, 3H), 5.82 (br. s., 1H), 6.69 - 6.84 (m, 3H), 6.84 - 6.96 (m, 3H), 7.19 (t, *J* = 8.0 Hz, 1H), 7.24 - 7.40 (m, 4H), 7.69 - 7.80 (m, 1H), 7.93 (s, 1H), 10.77 (s, 1H); MS(ESI) *m*/*z* 484 $[M + H]^+$.

4-Amino-2-phenyl-7,8-dihydro-1,6-naphthyridin-5(6*H*)-one (37). Typical procedure for Boc-deprotection and sulfide displacement with ammonia. (Scheme 1, conditions i and j). **Method 1ij.** Step 1. Trifluoroacetic acid (1 mL, 13 mmol) was added drop-wise to a solution of **12** (R^1 = Ph, 212 mg, 0.53 mmol) dissolved in 5 mL of dichloromethane and the mixture was allowed to stand at room temperature for 1 h. The mixture was diluted with 50 mL of chloroform and was evaporated to give a residue. Water (5 mL) was added and a solid precipitated. The acidic solution was basified to pH 10 with 4% w/v sodium carbonate solution and the mixture was sonicated to finely divide the solid, which was collected by filtration, washed twice with water and dried in a stream of air for 1 h to give *4-(methylsulfonyl)-2-phenyl-7,8-dihydro-1,6-naphthyridin-5(6H)-one* as a tan solid (160 mg, 0.53 mmol, 100% yield): ^{1}H NMR (200 MHz, DMSO-d_6) δ 3.21 (t, *J* = 5.1 Hz, 2H), 3.38 - 3.56 (m, 2H), 3.69 (s, 3H), 7.50-7.68 (m, 3H), 8.09 - 8.20 (m, 2H), 8.32 (s, 1H), 8.52 (br. s., 1H); MS(ESI) *m*/*z* 303 $[M + H]^+$.

Step 2. The sulfone (125 mg, 0.30 mmol) was suspended in 7N ammonia in methanol (2.00 mL, 14.00 mmol) and the mixture was heated in the microwave at 70 ºC for 2 h and at 100 ºC for 5 h. The solvent was evaporated and the crude was purified by reverse phase in the SP1 purification system to give **37** as a white solid (38 mg, 0.15 mmol, 52% yield), HPLC purity 98%: partial ^{1}H NMR (200 MHz, DMSO-d_6) δ 2.89 (t, *J* = 6.8 Hz, 2H), 3.37 (td, *J* = 6.6, 2.5 Hz, 2H), 7.03 (s, 1H), 7.36 - 7.54 (m, 3H), 7.79 (br. s., 1H), 7.94 (d, *J* = 5.9 Hz, 2H); MS(ESI) *m*/*z* 240 $[M + H]^+$.

3-[(5-Oxo-2-phenyl-5,6,7,8-tetrahydro-1,6-naphthyridin-4-yl)amino]benzonitrile (38). Method 1f. Pale yellow solid, HPLC purity 99%. 26% Yield from **12** (R^1 = Ph) and 3-cyanoaniline: ^{1}H NMR (200 MHz, $CDCl_3$) δ 3.20 (t, *J* = 6.8 Hz, 2H), 3.66 (td, *J* = 6.8, 2.5 Hz, 2H), 5.94 (br. s., 1H), 7.29 (s, 1H), 7.36 - 7.63 (m, 7H), 7.81 - 7.93 (m, 2H), 11.00 (s, 1H); MS(ESI) *m*/*z* 341 $[M + H]^+$.

4-[(3,5-Dimethoxyphenyl)amino]-2-phenyl-7,8-dihydro-1,6-naphthyridin-5(6*H*)-one (39). Typical procedure for direct sulfide displacement with amines and anilines under conventional heating and subsequent Boc-deprotection under thermal conditions (Scheme 1, conditions g). **Method 1g.** A mixture of **12** (R^1 = Ph, 80 mg, 0.19 mmol) and 3,5-dimethoxyaniline (145 mg, 0.95 mmol) suspended in 2 mL ethanol was heated at 70 ºC overnight in a capped vial. The contents of the vial were transferred to a microwave vessel and were heated at 160 ºC under microwave irradiation for 30 min. The solvent was concentrated under reduced pressure and the crude residue was purified by flash chromatography (gradient ethyl acetate-methanol) to give **39** as a pale yellow solid (14 mg, 0.035 mmol, 19% yield), HPLC purity 99%: ^{1}H NMR (200 MHz, $CDCl_3$) δ 3.17 (t, *J* = 6.6 Hz, 2H), 3.63 (td, *J* = 6.5, 2.0 Hz, 2H), 3.80 (s, 6H), 6.00 (br. s., 1H), 6.32 (s, 1H), 6.47 (d, *J* = 2.0 Hz, 2H), 7.33 - 7.51 (m, 4H), 7.80 - 7.94 (m, 2H), 10.75 (s, 1H); MS(ESI) *m*/*z* 376 $[M + H]^+$.

4-{[3-(Hydroxymethyl)phenyl]amino}-2-phenyl-7,8-dihydro-1,6-naphthyridin-5(6*H*)-one (40). Method 1g. Pale yellow solid, HPLC purity 96%. 40% Yield from **12** (R^1 = Ph) and 3-aminobenzylalcohol: ^{1}H NMR (200 MHz, $CDCl_3$) δ 3.15 (t, *J* = 6.8 Hz, 2H), 3.61 (t, *J* = 6.8 Hz, 2H), 4.69 (s, 2H), 7.28 (app d, *J* = 7.0 Hz, 4H), 7.33 - 7.47 (m, 4H), 7.71 - 7.86 (m, 2H), 10.75 (br. s., 1H); MS(ESI) *m*/*z* 346 $[M + H]^+$.

4-{[4-(2-Hydroxyethyl)phenyl]amino}-2-phenyl-7,8-dihydro-1,6-naphthyridin-5(6*H*)-one (41). Method 1g, HPLC purity 90%. Pale yellow solid. 51% Yield from **12** (R^1 = Ph) and 2-(4-aminophenyl)ethanol: ^{1}H NMR (200 MHz, $CDCl_3$) δ 2.91 (t, *J* = 6.4 Hz, 2H), 3.21 (t, *J* = 6.6 Hz, 2H), 3.65 (td, *J* = 6.0, 2.0 Hz, 2H), 3.91 (t, *J* = 6.4 Hz, 2H), 5.87 (br. s., 1H), 7.23 – 7.30 (m, 4H), 7.34 - 7.51 (m, 4H), 7.80 - 7.93 (m, 2H), 10.79 (br. s., 1H); MS(ESI) *m*/*z* 360 $[M + H]^+$.

4-({4-[(2*R*)-2,3-dihydroxypropyl]phenyl}amino)-2-phenyl-7,8-dihydro-1,6-naphthyridin-5(6*H*)-one (42). 2,2-Dimethyl-4-(4-nitrobenzyl)-1,3-dioxolane (1.15 g, 4.85 mmol) was dissolved in 50 mL of ethanol and 10% Pd/C (0.26 g, 0.24 mmol) was added. The mixture was stirred under nitrogen atmosphere at 20 psi for 2 h. The catalyst was filtered and the solvent was evaporated to give *{4-[(2,2-dimethyl-1,3-dioxolan-4-yl)methyl]phenyl}amine* as an orange solid (965 mg, 4.51 mmol, 96% yield): ^{1}H NMR (200 MHz, $CDCl_3$) δ 1.36 (s, 3H), 1.44 (s, 3H), 2.50 - 2.78 (m, 1H), 2.86 - 3.06 (m, 1H), 3.54 - 3.73 (m, 1H), 3.95 (dd, *J* = 8.2, 5.9 Hz, 1H), 4.14 - 4.40 (m, 1H), 6.68 (d, *J* = 8.4 Hz, 2H), 7.02 (d, *J* = 8.4 Hz, 2H); MS(ESI) *m*/*z* 208 $[M + H]^+$. **42**: Method 1h. Pale yellow solid, HPLC purity 98%. 19% Yield from **12** (R^1 = Ph) and {4-[(2,2-dimethyl-1,3-dioxolan-4-yl)methyl]phenyl}amine: ^{1}H NMR (400 MHz, DMSO-d_6) δ 2.54 (dd, *J* = 13.5, 8.5 Hz, 1H), 2.80 (dd, *J* = 13.5, 4.5 Hz, 1H), 3.00 (t, *J* = 6.7 Hz, 2H), 3.46 (td, *J* = 6.5, 2.5 Hz, 2H), 3.60 - 3.70 (m, 1H), 4.58 - 4.64 (m, 2H), 7.22 - 7.27 (m, 2H), 7.27 - 7.32 (m, 3H), 7.39 - 7.51 (m, 3H), 7.89 (d, *J* = 6.3 Hz, 2H), 8.16 (br. s., 1H), 11.03 (s, 1H); MS(ESI) *m*/*z* 390 $[M + H]^+$.

2-Methoxy-4-[(5-oxo-2-phenyl-5,6,7,8-tetrahydro-1,6-naphthyridin-4-yl)amino]benzoic acid (43). Method 1h, HPLC purity 87%. Pale brown solid. 16% Yield from **12** (R^1 = Ph) and 4-amino-2-methoxybenzoic acid: ^{1}H NMR (200 MHz, $CDCl_3$) δ 3.17 (t, *J* = 6.6 Hz, 2H), 3.63 (td,

J = 6.8, 2.7 Hz, 2H), 3.82 (s, 3H), 5.90 (br. s., 1H), 6.76 (dd, *J* = 8.2, 2.5 Hz, 1H), 6.84 (s, 1H), 6.91 (d, *J* = 7.8 Hz, 1H), 7.30 - 7.49 (m, 4H), 7.80 - 7.92 (m, 2H), 10.76 (s, 1H); MS(ESI) *m*/*z* 390 $[M + H]^+$.

4-[(5-Oxo-2-phenyl-5,6,7,8-tetrahydro-1,6-naphthyridin-4-yl)amino]benzamide (44). Method 1h. Yellow solid, HPLC purity 97%. 75% Yield from **12** (R^1 = Ph) and 4-aminobenzamide: ^{1}H NMR (400 MHz, DMSO-d_6) δ 3.13 (t, *J* = 6.8 Hz, 2H), 3.60 (t, *J* = 6.8 Hz, 2H), 6.66 (d, *J* = 8.6 Hz, 2H), 7.37 - 7.42 (m, 2H), 7.43 - 7.49 (m, 2H), 7.63 (d, *J* = 8.6 Hz, 2H), 7.78 (s, 1H), 7.78 – 7.82 (m, 1H), 7.95 (d, *J* = 8.6 Hz, 2H); MS(ESI) *m*/*z* 359 $[M + H]^+$.

3-[(5-Oxo-2-phenyl-5,6,7,8-tetrahydro-1,6-naphthyridin-4-yl)amino]benzamide (45). Method 1h. Pale yellow solid, HPLC purity 98%. 46% Yield from **12** (R^1 = Ph) and 3-aminobenzamide: ^{1}H NMR (200 MHz, DMSO-d_6) δ 3.03 (t, *J* = 6.8 Hz, 2H), 3.48 (t, *J* = 6.8 Hz, 2H), 7.36 (s, 1H), 7.41 - 7.50 (m, 4H), 7.50 - 7.57 (m, 2H), 7.67 - 7.75 (m, 1H), 7.83 (s, 1H), 7.88 - 7.98 (m, 2H), 8.06 (br. s., 1H), 8.23 (s, 1H), 11.21 (s, 1H); MS(ESI) *m*/*z* 359 $[M + H]^+$.

4-[(4-Methylpyridin-3-yl)amino]-2-phenyl-7,8-dihydro-1,6-naphthyridin-5(6*H*)-one (46). Typical procedure for palladium-catalyzed aminations (Scheme 1, conditions k and Scheme 2, conditions c). **Method 1k.** Compound **37** (45 mg, 0.19 mmol) was dissolved in 10 mL of dioxane in a sealed tube. The mixture was subjected to three cycles of evacuation-backfilling with argon and 3-bromo-4-methylpyridine (26 mg, 0.23 mmol), cesium carbonate (85 mg, 0.26 mmol), bis(diphenylphosphino)-9,9-dimethylxanthene (22 mg, 0.04 mmol) and tris(dibenzylidene acetone)dipalladium(0) (17 mg, 0.02 mmol) were added. The mixture was subjected again to three cycles of evacuation-backfilling and the mixture was stirred at 120 ºC under argon atmosphere overnight. The solvent was evaporated and dichloromethane and water

were added. The organic layer was washed with water (x2), dried with magnesium sulfate, filtered and evaporated The residue was purified by reverse phase using the SP1 purification system to give **46** as a white solid (26 mg, 0.078 mmol, 42% yield), HPLC purity 100%: partial ^{1}H NMR (200 MHz, $CDCl_3$) δ 2.33 (s, 3H), 3.21 (t, *J* = 6.8 Hz, 2H), 3.67 (td, *J* = 6.7, 2.5 Hz, 2H), 5.83 (br. s., 1H), 6.89 (s, 1H), 7.34 - 7.45 (m, 3H), 7.77 - 7.88 (m, 2H), 8.40 (br. s., 1H), 8.62 (br. s., 1H), 10.66 (s, 1H); MS(ESI) *m*/*z* 331 $[M + H]^+$.

2-Phenyl-4-[(pyridin-4-ylmethyl)amino]-7,8-dihydro-1,6-naphthyridin-5(6*H*)-one (47). Method 1g. White solid, HPLC purity 93%. 23% Yield from **12** (R^1 = Ph) and 4-aminomethylpyridine: partial ^{1}H NMR (400 MHz, DMSO-d_6) δ 2.95 (t, *J* = 6.8 Hz, 2H), 4.70 (d, *J* = 6.3 Hz, 2H), 6.94 (s, 1H), 7.36 (d, *J* = 5.1 Hz, 2H), 7.38 - 7.47 (m, 3H), 7.95 (app d, *J* = 7.5 Hz, 3H), 8.53 (d, *J* = 4.7 Hz, 2H), 9.59 (t, *J* = 6.1 Hz, 1H); MS(ESI) *m*/*z* 331 $[M + H]^+$.

2-Phenyl-4-[(2-pyridin-4-ylethyl)amino]-7,8-dihydro-1,6-naphthyridin-5(6*H*)-one (48). Method 1h. White solid, HPLC purity 98%. 19% Yield from **12** (R^1 = Ph) and 2-(pyridin-4-yl)ethylamine: ^{1}H NMR (200 MHz, $CDCl_3$) δ 3.01 (t, *J* = 7.2 Hz, 2H), 3.11 (t, *J* = 7.0 Hz, 2H), 3.45 - 3.69 (m, 4H), 5.85 (br. s., 1H), 6.81 (s, 1H), 7.21 (d, *J* = 5.5 Hz, 2H), 7.37 - 7.58 (m, 3H), 7.93 (d, *J* = 7.8 Hz, 2H), 8.56 (d, *J* = 5.5 Hz, 2H), 9.09 (t, *J* = 4.7 Hz, 1H); MS(ESI) *m*/*z* 345 $[M + H]^+$.

4-(1-Naphthylamino)-2-phenyl-7,8-dihydro-1,6-naphthyridin-5(6*H*)-one (49). Method 1h. Pale yellow solid, HPLC purity 98%. 37% Yield from **12** (R^1 = Ph) and 1-aminonaphthalene: ^{1}H NMR (200 MHz, $CDCl_3$) δ 3.22 (t, *J* = 6.6 Hz, 2H), 3.68 (td, *J* = 6.8, 2.5 Hz, 2H), 6.10 (br. s., 1H), 7.00 (s, 1H), 7.27 - 7.40 (m, 3H), 7.43 - 7.61 (m, 4H), 7.64 - 7.85 (m, 3H), 7.84 - 7.98 (m, 1H), 8.04 - 8.16 (m, 1H), 11.09 (br. s., 1H); MS(ESI) *m*/*z* 366 $[M + H]^+$.

2-Phenyl-4-(quinolin-5-ylamino)-7,8-dihydro-1,6-naphthyridin-5(6*H*)-one (50). Method 1h. Pale yellow solid, HPLC purity 98%. 22% Yield from **12** (R^1 = Ph) and 5-aminoquinoline: ^{1}H NMR (200 MHz, $CDCl_3$) δ 3.23 (t, *J* = 6.6 Hz, 2H), 3.69 (t, *J* = 6.4 Hz, 2H), 6.07 (br. s., 1H), 6.99 (s, 1H), 7.30 - 7.52 (m, 5H), 7.57 - 7.68 (m, 1H), 7.68 - 7.85 (m, 2H), 8.07 (d, *J* = 8.6 Hz, 1H), 8.44 (d, *J* = 8.2 Hz, 1H), 8.98 (d, *J* = 2.7 Hz, 1H), 11.15 (s, 1H); MS(ESI) *m*/*z* 367 $[M + H]^+$.

4-(Isoquinolin-5-ylamino)-2-phenyl-7,8-dihydro-1,6-naphthyridin-5(6*H*)-one (51). Method 1h. Pale yellow solid, HPLC purity 100%. 7% Yield from **12** (R^1 = Ph) and 5-aminoisoquinoline: ^{1}H NMR (200 MHz, $CDCl_3$) δ 3.23 (t, *J* = 6.6 Hz, 2H), 3.70 (td, *J* = 6.6, 2.3 Hz, 2H), 5.93 (br. s., 1H), 7.02 (s, 1H), 7.32 - 7.42 (m, 3H), 7.66 (t, *J* = 8.0 Hz, 1H), 7.72 - 7.82 (m, 3H), 7.84 - 7.96 (m, 2H), 8.57 (d, *J* = 5.9 Hz, 1H), 9.33 (s, 1H), 11.21 (s, 1H); MS(ESI) *m*/*z* 367 $[M + H]^+$.

2-Phenyl-4-(quinolin-6-ylamino)-7,8-dihydro-1,6-naphthyridin-5(6*H*)-one (52). Method 1h. Pale yellow solid, HPLC purity 100%. 11% Yield from **12** (R^1 = Ph) and 6-aminoquinoline: ^{1}H NMR (200 MHz, $CDCl_3$) δ 3.21 (t, *J* = 6.6 Hz, 2H), 3.67 (td, *J* = 6.6, 2.5 Hz, 2H), 6.02 (br. s., 1H), 7.37 – 7.48 (m, 5H), 7.63 - 7.77 (m, 2H), 7.87 (app dd, *J* = 6.0, 2.5 Hz, 2H), 8.13 (t, *J* = 8.6 Hz, 2H), 8.88 (d, *J* = 2.7 Hz, 1H), 11.06 (s, 1H); MS(ESI) *m*/*z* 367 $[M + H]^+$.

2-Phenyl-4-(1H-pyrazolo[3,4-b]pyridin-3-ylamino)-7,8-dihydro-1,6-naphthyridin-5(6*H*)-one (53). 2-Chloronicotinonitrile (0.75 g, 5.30 mmol), copper iodide (I) (50 mg, 0.05 mmol), cesium carbonate (2.59 g, 7.96 mmol) and 1,10-phenanthroline (96 mg, 0.53 mmol) were suspended in 20 mL of dimethylformamide. Hydrazine hydrate (1.6 mL, 31.83 mmol) was added and the mixture was stirred at 60 ºC overnight. The mixture was cooled to room

temperature, water was added and the aqueous phase was extracted with dichloromethane (x3). The combined organic layers were dried with magnesium sulfate, filtered and evaporated. The crude was purified by column chromatography using the SP1 Purification system (methanol-dichloromethane gradient) to give *1H-pyrazolo[3,4-b]pyridin-3-amine* as a yellow solid (0.34 g, 2.51 mmol, 47% yield): ^{1}H NMR (200 MHz, DMSO-d_6) δ 5.55 (s, 2H), 6.94 (dd, *J* = 7.8, 4.7 Hz, 1H), 8.10 (dd, *J* = 7.8, 1.6 Hz, 1H), 8.33 (dd, *J* = 4.3, 1.6 Hz, 1H), 11.91 (br. s., 1H); MS(ESI) *m*/*z* 135 $[M + H]^+$. **53**: Method 1h. Pale yellow solid, HPLC purity 99%. 53% Yield from **12** (R^1 = Ph) and 1H-pyrazolo[3,4-b]pyridin-3-amine: ^{1}H NMR (200 MHz, DMSO-d_6) δ 3.08 (t, *J* = 6.4 Hz, 2H), 3.51 (t, *J* = 6.6 Hz, 2H), 7.23 (dd, *J* = 8.0, 4.5 Hz, 1H), 7.39 - 7.62 (m, 3H), 8.02 (d, *J* = 5.9 Hz, 2H), 8.10 (d, *J* = 8.2 Hz, 1H), 8.34 (br. s., 1H), 8.58 (d, *J* = 4.3 Hz, 1H), 8.67 (s, 1H), 12.37 (s, 1H), 13.19 (s, 1H); MS(ESI) *m*/*z* 356 $[M + H]^+$.

4-[(1-Methyl-1H-pyrazolo[3,4-b]pyridin-3-yl)amino]-2-phenyl-7,8-dihydro-1,6-naphthyridin-5(6*H*)-one (54). Method 1h. Pale yellow solid, HPLC purity 100%. 53% Yield from **12** (R^1 = Ph) and 1-methyl-1H-pyrazolo[3,4-b]pyridin-3-amine (prepared as above from 2-chloronicotinonitrile and methylhydrazine): ^{1}H NMR (200 MHz, $CDCl_3$) δ 3.25 (t, *J* = 6.8 Hz, 2H), 3.68 (td, *J* = 6.8, 2.5 Hz, 2H), 4.14 (s, 3H), 5.81 (br. s., 1H), 7.10 (dd, *J* = 7.8, 4.7 Hz, 1H), 7.37 - 7.57 (m, 3H), 8.07 (app t, *J* = 8.4 Hz, 3H), 8.57 (d, *J* = 4.3 Hz, 1H), 8.63 (s, 1H), 11.94 (s, 1H); MS(ESI) *m*/*z* 371 $[M + H]^+$.

2-Phenyl-4-[(1-phenyl-1H-pyrazolo[3,4-b]pyridin-3-yl)amino]-7,8-dihydro-1,6-naphthyridin-5(6*H*)-one (55). Method 1h. Pale yellow solid, HPLC purity 100%. 40% Yield from **12** (R^1 = Ph) and 1-phenyl-1H-pyrazolo[3,4-b]pyridin-3-amine (prepared as above from 2-chloronicotinonitrile and phenylhydrazine): ^{1}H NMR (200 MHz, $CDCl_3$) δ 3.27 (t, *J* = 6.8 Hz,

2H), 3.69 (td, J = 6.8, 2.3 Hz, 2H), 5.90 (br. s., 1H), 7.10 - 7.33 (m, 2H), 7.41 - 7.63 (m, 5H), 8.17 (app t, J = 7.0 Hz, 3H), 8.41 (d, J = 8.2 Hz, 2H), 8.66 (d, J = 4.3 Hz, 1H), 9.08 (s, 1H), 12.27 (s, 1H); MS(ESI) m/z 433 $[M + H]^+$.

4-[(1-Oxidoquinolin-5-yl)amino]-2-phenyl-7,8-dihydro-1,6-naphthyridin-5(6*H*)-one (56). 5-Bromoquinoline (0.50 g, 2.40 mmol) was dissolved in 20 mL dichloromethane and was cooled to 5 ºC in an ice-bath. *meta*-Chloroperbenzoic acid (max purity 77%, 0.88 g, 3.60 mmol) was added and the mixture was stirred for 30 min at 5 ºC. The mixture was then stirred at room temperature for 2 h. The organics were washed three times with 4% w/v sodium carbonate solution, once with brine and dried over sodium sulfate. The organics were filtered and evaporated to give *5-bromoquinoline 1-oxide* as a brown solid (0.48 g, 0.21 mmol, 86% yield): ^{1}H NMR (200 MHz, $CDCl_3$) δ 7.40 (dd, J = 8.8, 6.1 Hz, 1H), 7.60 (t, J = 8.2 Hz, 1H), 7.93 (d, J = 7.4 Hz, 1H), 8.11 (d, J = 9.0 Hz, 1H), 8.58 (d, J = 6.2 Hz, 1H), 8.76 (d, J = 8.6 Hz, 1H); MS(ESI) m/z 226 $[M + H]^+$. **56**: Method 1k. Yellow solid, HPLC purity 99%. 35% Yield from **37** and 5-bromoquinoline 1-oxide: ^{1}H NMR (200 MHz, DMSO-d_6) δ 3.06 (t, J = 6.6 Hz, 2H), 3.52 (td, J = 6.5, 2.0 Hz, 2H), 7.21 (s, 1H), 7.35 - 7.47 (m, 3H), 7.53 (dd, J = 8.8, 6.1 Hz, 1H), 7.81 - 7.97 (m, 5H), 8.33 (br. s., 1H), 8.43 (t, J = 4.9 Hz, 1H), 8.66 (d, J = 5.9 Hz, 1H), 11.68 (s, 1H); MS(ESI) m/z 383 $[M + H]^+$.

4-[(3-Methoxyphenyl)amino]-2-phenyl-7,8-dihydropyrido[4,3-d]pyrimidin-5(6*H*)-one (57). Step 1. Phenylamidine hydrochloride (0.25 g, 1.58 mmol) was suspended in 5 mL toluene and 1 mL dimethylformamide. Sodium hydride (60% dispersion in oil, 0.125 g, 3.15 mmol) was added and the mixture was stirred for 5 min. A solution of **9** (0.50 g, 1.58 mmol) dissolved in 4 mL dimethylformamide was added and the mixture was stirred at 100 ºC for 2 d. The mixture was

evaporated and the crude residue purified by reverse-phase chromatography using the SP1 Purification system to give tert-*butyl 4-(methylthio)-5-oxo-2-phenyl-7,8-dihydropyrido[4,3-d]pyrimidine-6(5H)-carboxylate* as a colourless oil (60 mg, 0.15 mmol, 9%): MS(ESI) *m*/*z* 373 $[M + H]^+$.

Step 2. The sulfide (60 mg, 0.15 mmol) was dissolved in 2 mL dichloromethane and was cooled to 5 ºC in an ice-bath. *meta*-Chloroperbenzoic acid (max purity 77%, 0.10 g, 0.45 mmol) was added and the mixture was stirred for 30 min at 5 ºC. The mixture was then stirred at room temperature for 2 h. The organics were washed three times with 4% w/v sodium carbonate solution, once with brine and dried over sodium sulfate. The organics were filtered and evaporated to give a crude sample of *4-(methylsulfonyl)-2-phenyl-7,8-dihydropyrido[4,3-d]pyrimidin-5(6H)-one* as a colourless oil (84 mg, purity 70% by HPLC). Used as such without further purification: MS(ESI) *m*/*z* 305 $[M + H]^+$. **57**: Method 1h. Pale yellow solid, HPLC purity 99%. 83% Yield from the crude 4-(methylsulfonyl)-2-phenyl-7,8-dihydropyrido[4,3-d]pyrimidin-5(6H)-one and 3-methoxyaniline: ^{1}H NMR (200 MHz, DMSO-d_6) δ 3.01 (t, *J* = 6.8 Hz, 2H), 3.50 (td, *J* = 6.5, 2.0 Hz, 2H), 3.83 (s, 3H), 6.71 (d, *J* = 7.8 Hz, 1H), 7.21 (d, *J* = 8.0 Hz, 1H), 7.33 (t, *J* = 7.8 Hz, 1H), 7.47 - 7.71 (m, 4H), 8.26 - 8.53 (m, 3H), 11.61 (s, 1H); MS(ESI) *m*/*z* 347 $[M + H]^+$.

4-[(3-Methoxyphenyl)amino]-7-methyl-2-phenyl-7,8-dihydro-1,6-naphthyridin-5(6*H*)-one (58). Method 1h. White solid, HPLC purity 94%. 56% yield from *tert*-butyl 7-methyl-4-(methylsulfonyl)-5-oxo-2-phenyl-7,8-dihydro-1,6-naphthyridine-6(5H)-carboxylate and 3-methoxyaniline: ^{1}H NMR (200 MHz, $CDCl_3$) δ 1.39 (d, *J* = 6.6 Hz, 3H), 2.93 (dd, *J* = 16.0, 11.0 Hz, 1H), 3.17 (dd, *J* = 16.0, 5.0 Hz, 1H), 3.82 (s, 3H), 3.95 (ddt, *J* = 11.0, 5.0, 6.5 Hz, 1H),

5.60 (br. s., 1H), 6.76 (d, *J* = 8.6 Hz, 1H), 6.84 (s, 1H), 6.92 (d, *J* = 8.6 Hz, 1H), 7.30 - 7.49 (m, 5H), 7.83 - 7.93 (m, 2H), 10.78 (s, 1H); MS(ESI) *m*/*z* 360 $[M + H]^+$.

4-[(3-Methoxyphenyl)amino]-8-methyl-2-phenyl-7,8-dihydro-1,6-naphthyridin-5(6*H*)-one (59). Method 1h. Brown solid, HPLC purity 96%. 75% yield from *tert*-butyl 8-methyl-4-(methylsulfonyl)-5-oxo-2-phenyl-7,8-dihydro-1,6-naphthyridine-6(5H)-carboxylate and 3-methoxyaniline: ^{1}H NMR (200 MHz, $CDCl_3$) δ 1.47 (d, *J* = 6.6 Hz, 3H), 3.14 - 3.26 (m, 1H), 3.26 - 3.40 (m, 1H), 3.74 (ddd, *J* = 12.0, 5.0, 2.3 Hz, 1H), 3.82 (s, 3H), 5.77 (br. s., 1H), 6.75 (dd, *J* = 8.2, 2.2 Hz, 1H), 6.84 (s, 1H), 6.91 (d, *J* = 7.8 Hz, 1H), 7.31 (t, *J* = 7.8 Hz, 1H), 7.35 - 7.47 (m, 4H), 7.86 - 7.97 (m, 2H), 10.80 (s, 1H); MS(ESI) *m*/*z* 360 $[M + H]^+$.

4-((3-Methoxyphenyl)amino)-6-phenylnicotinamide (60). Step 1. 2-Bromo-5-methyl-4-nitropyridine (3.50 g, 16.1 mmol), phenylboronic acid (2.36 g, 19.4 mmol) and [1,1′-bis(diphenylphosphino)ferrocene]dichloropalladium(II), complex with dichloro-methane (0.66 g, 0.81 mmol) were dissolved in 250 mL dioxane. 25 mL 2M Aqueous sodium carbonate solution was added and the reaction vessel was subject to two cycles of evacuation-backfilling with argon. The mixture was stirred under argon at heated at 90 ºC for 4 h. The mixture was allowed to cool, was diluted with ethyl acetate and the organics were washed twice with water and once with brine. The organics were dried over magnesium sulfate, filtered and evaporated. The residue was partially purified by flash chromatography (dichloromethane) to give a crude sample of *5-methyl-4-nitro-2-phenylpyridine* (3 g, 70% purity by HPLC).

Step 2. The crude sample of 5-methyl-4-nitro-2-phenylpyridine (3 g) was dissolved in 20 mL pyridine and 10 mL water. Potassium permanganate (7.9 g, 50 mmol) was added portion-wise and with stirring. The mixture was stirred at reflux overnight. The mixture was allowed to cool,

further potassium permanganate (7.9 g, 50 mmol) was added portion-wise and the mixture was stirred at reflux for 6 h. The mixture was cooled and filtered through a plug of Celite, washing the Celite first with water and then ethyl acetate. The biphasic filtrate was separated and the aqueous was adjusted to pH 4-5 with 2M hydrochloric acid. The aqueous was extracted three times with ethyl acetate, the combined organics were washed with brine and dried over magnesium sulfate. Evaporation gave *4-nitro-6-phenylnicotinic acid* (1.3 g, 5.4 mmol, 34% yield over two steps): ^{1}H NMR (200 MHz, $CDCl_3$) δ 7.48 - 7.66 (m, 3H), 7.95 (s, 1H), 8.11 (t, *J* = 7.6 Hz, 2H), 9.33 (s, 1H); MS(ESI) *m*/*z* 243 $[M - H]^+$.

Step 3. 4-Nitro-6-phenylnicotinic acid (1.3 g, 5.4 mmol) was dissolved in 30 mL dimethylformamide. Potassium carbonate (1.49 g, 10.8 mmol) and ethyl bromide (0.40 mL, 5.4 mmol) were added and the mixture was stirred at 50 ºC for 2 h. The mixture was diluted with water and was extracted three times with ethyl acetate, the combined organics were washed with brine, dried over magnesium sulfate and evaporated. The residue was purified by flash chromatography (dichloromethane-hexane, gradient) to give *ethyl 4-nitro-6-phenylnicotinate* (0.8 g, 2.9 mmol, 54% yield): ^{1}H NMR (200 MHz, $CDCl_3$) δ 1.39 (t, *J* = 7.0 Hz, 3H), 4.44 (q, *J* = 7.0 Hz, 2H), 7.47 - 7.63 (m, 3H), 7.99 (s, 1H), 8.02 - 8.14 (m, 2H), 9.19 (s, 1H); MS(ESI) *m*/*z* 273 $[M + H]^+$.

Step 4. Ethyl 4-nitro-6-phenylnicotinate (0.8 g, 2.9 mmol) was dissolved in 40 mL ethanol. Palladium on carbon (10%, 160 mg) was added and the mixture was agitated under hydrogen atmosphere at 30 psi for 3 h. The mixture was filtered through a plug of Celite and the filtrate was evaporated to give ethyl *4-amino-6-phenylnicotinate* (0.55 g, 2.3 mmol, 74% yield): ^{1}H

NMR (200 MHz, $CDCl_3$) δ 1.41 (t, *J* = 7.2 Hz, 3H), 4.38 (q, *J* = 7.0 Hz, 2H), 6.23 (br. s., 2H), 6.93 (s, 1H), 7.39 - 7.54 (m, 3H), 7.90 - 8.00 (m, 2H), 9.01 (s, 1H); MS(ESI) *m*/*z* 243 $[M + H]^+$.

Step 5. A mixture of ethyl 4-amino-6-phenylnicotinate (100 mg, 0.41 mmol), 3-bromoanisole (0.078 mL, 0.62 mmol), potassium carbonate (120 mg, 0.87 mmol), copper(I) iodide (8 mg, 0.04 mmol) and N,N'-dimethylethane-1,2-diamine (0.009 mL, 0.08 mmol) were suspended in 2 mL anhydrous dioxane in a pressure tube. The mixture was subject to two cycles of evacuation-backfilling with argon, the tube was sealed and the mixture was stirred at 140 ºC overnight. The mixture was diluted with ethyl acetate and was washed with ammonium hydroxide solution and with brine. The organics were dried over magnesium sulfate, evaporated and the residue purified by reverse-phase chromatography to give *ethyl 4-(3-methoxyphenylamino)-6-phenylnicotinate* (119 mg, 0.34 mmol, 83% yield): ^{1}H NMR (200 MHz, $CDCl_3$) δ 1.44 (t, *J* = 7.2 Hz, 3H), 3.83 (s, 3H), 4.43 (q, *J* = 7.0 Hz, 2H), 6.76 - 6.86 (m, 2H), 6.92 (d, *J* = 8.6 Hz, 1H), 7.29 - 7.39 (m, 1H), 7.38 - 7.49 (m, 4H), 7.84 - 7.96 (m, 2H), 9.12 (s, 1H), 9.96 (br. s., 1H); MS(ESI) *m*/*z* 349 $[M + H]^+$.

Step 6. Ethyl 4-(3-methoxyphenylamino)-6-phenylnicotinate (119 mg, 0.34 mmol) was dissolved in 5 mL tetrahydrofuran and 5 mL water. Lithium hydroxide hydrate (72 mg, 1.7 mmol) was added and the mixture was stirred overnight. The THF was evaporated and the aqueous solution was purified directly by reverse-phase chromatography to give *4-(3-methoxyphenylamino)-6-phenylnicotinic acid* (61 mg, 0.19 mmol, 56% yield) as a white solid: ^{1}H NMR (200 MHz, DMSO-d_6) δ 3.79 (s, 3H), 6.82 (dd, *J* = 8.0, 2.0 Hz, 1H), 6.93 - 7.07 (m, 2H), 7.38 (t, *J* = 8.0 Hz, 1H), 7.43 - 7.53 (m, 4H), 7.83 - 7.96 (m, 2H), 8.93 (s, 1H), 10.38 (br. s., 1H); MS(ESI) *m*/*z* 319 $[M - H]^+$.

Step 7. 4-(3-Methoxyphenylamino)-6-phenylnicotinic acid (50 mg, 0.16 mmol) was dissolved in 2 mL dimethylformamide. *N*-Hydroxybenzotriazole (HOBt, 32 mg, 0.24 mmol), 1-ethyl-3-(3-dimethylaminopropyl)carbodiimide (EDC, 45 mg, 0.23 mmol) and concentrated ammonia solution (0.013 mL, 0.33 mmol) were added and the mixture was stirred overnight at room temperature. The mixture was purified directly by reverse-phase chromatography to give **60** as a white solid (8 mg, 0.025 mmol, 16% yield), HPLC purity 97%: ^{1}H NMR (400 MHz, DMSO-d_6) δ 3.72 (s, 3H), 6.75 (dd, J = 8.2, 2.3 Hz, 1H), 6.80 (s, 1H), 6.89 (d, J = 7.8 Hz, 1H), 7.33 (t, J = 8.0 Hz, 1H), 7.39 (s, 1H), 7.39 - 7.47 (m, 4H), 7.78 (d, J = 8.2 Hz, 2H), 8.28 (br. s., 1H), 8.73 (s, 1H), 10.32 (s, 1H); MS(ESI) m/z 320 $[M + H]^+$.

6-Phenyl-4-(quinolin-5-ylamino)nicotinamide (61). Step 1. A mixture of ethyl 4-amino-6-phenylnicotinate (see **60**, step 4, 100 mg, 0.41 mmol), 5-bromoquinoline (129 mg, 0.62 mmol), potassium carbonate (120 mg, 0.87 mmol), copper(I) iodide (8 mg, 0.04 mmol) and N,N'-dimethylethane-1,2-diamine (0.009 mL, 0.08 mmol) were suspended in 2 mL anhydrous dioxane in a pressure tube. The mixture was subject to two cycles of evacuation-backfilling with argon, the tube was sealed and the mixture was stirred at 140 ºC overnight. The mixture was diluted with ethyl acetate and was washed with ammonium hydroxide solution and with brine. The organics were dried over magnesium sulfate, evaporated and the residue purified by reverse-phase chromatography to give *ethyl 6-phenyl-4-(quinolin-5-ylamino)nicotinate* (106 mg, 0.29 mmol, 70% yield): ^{1}H NMR (200 MHz, $CDCl_3$) δ 1.49 (t, J = 7.0 Hz, 3H), 4.48 (q, J = 7.0 Hz, 2H), 7.01 (s, 1H), 7.32 - 7.40 (m, 3H), 7.46 (dd, J = 8.4, 4.1 Hz, 1H), 7.58 - 7.67 (m, 1H), 7.69 - 7.78 (m, 2H), 7.80 (t, J = 7.3 Hz, 1H), 8.11 (d, J = 8.6 Hz, 1H), 8.38 (d, J = 8.2 Hz, 1H), 9.00 (d, J = 2.3 Hz, 1H), 9.17 (s, 1H), 10.15 (s, 1H); MS(ESI) m/z 370 $[M + H]^+$.

Step 2. Ethyl 6-phenyl-4-(quinolin-5-ylamino)nicotinate (106 mg, 0.29 mmol) was dissolved in 5 mL tetrahydrofuran and 5 mL water. Lithium hydroxide hydrate (60 mg, 1.4 mmol) was added and the mixture was stirred overnight. The THF was evaporated and the aqueous solution was purified directly by reverse-phase chromatography to give *6-phenyl-4-(quinolin-5-ylamino)nicotinic acid* (86 mg, 0.25 mmol, 88% yield) as a yellow solid: ^{1}H NMR (200 MHz, DMSO-d_6) δ 7.12 (s, 1H), 7.33 - 7.48 (m, 3H), 7.60 (dd, J = 8.6, 3.9 Hz, 1H), 7.71 - 7.93 (m, 4H), 7.94 - 8.05 (m, 1H), 8.40 (d, J = 8.2 Hz, 1H), 8.98 (s, 2H); MS(ESI) m/z 340 $[M - H]^+$.

Step 3. 6-Phenyl-4-(quinolin-5-ylamino)nicotinic acid (60 mg, 0.18 mmol) was suspended in 6 mL dimethylformamide. HOBt (35 mg, 0.26 mmol), EDC (50 mg, 0.26 mmol) and concentrated ammonia solution (0.014 mL, 0.33 mmol) were added and the mixture was stirred overnight at room temperature. The mixture was purified directly by reverse-phase chromatography to give **61** as a white solid (50 mg, 0.15 mmol, 84% yield), HPLC purity 93%: ^{1}H NMR (200 MHz, DMSO-d_6) δ 7.21 (s, 1H), 7.34 - 7.47 (m, 3H), 7.61 (dd, J = 8.4, 4.1 Hz, 1H), 7.72 - 7.87 (m, 5H), 7.94 (t, J = 8.8 Hz, 1H), 8.32 - 8.45 (m, 2H), 8.91 - 9.04 (m, 2H), 11.19 (s, 1H); MS(ESI) m/z 341 $[M + H]^+$.

***N*-Methyl-6-phenyl-4-(quinolin-5-ylamino)nicotinamide (62).** 6-Phenyl-4-(quinolin-5-ylamino)nicotinic acid (see **61**, step 2, 70 mg, 0.21 mmol) was suspended in 2 mL dimethylformamide. HOBt (42 mg, 0.31 mmol), EDC (59 mg, 0.31 mmol) and methylamine hydrochloride (29 mg, 0.43 mmol) were added and the mixture was stirred overnight at room temperature. The mixture was purified directly by reverse-phase chromatography to give **62** as a white solid (63 mg, 0.18 mmol, 87% yield), HPLC purity 100%; ^{1}H NMR (200 MHz, DMSO-d_6) δ 2.88 (d, J = 4.3 Hz, 3H), 7.25 (s, 1H), 7.36 - 7.49 (m, 3H), 7.62 (dd, J = 8.4, 4.1 Hz, 1H),

7.76 (d, *J* = 7.5 Hz, 1H), 7.79 - 7.90 (m, 3H), 7.95 (d, *J* = 7.5 Hz, 1H), 8.39 (d, *J* = 8.2 Hz, 1H), 8.82 - 8.94 (m, 2H), 8.98 (dd, *J* = 4.2, 1.6 Hz, 1H), 10.98 (s, 1H); MS(ESI) *m*/*z* 355 $[M + H]^+$.

(5*Z*)-2-(3-Methoxyphenyl)-4-[(3-methoxyphenyl)amino]-7,8-dihydro-1,6-naphthyridin-5(6*H*)-one oxime (63). Step 1. Diisopropylethylamine (0.20 mL, 1.15 mmol) and diphosphorous pentasulfide (110 mg, 0.34 mmol) were added to a solution of **24** (55 mg, 0.15 mmol) dissolved in 2 mL of warm dioxane. The mixture was stirred at 100 ºC overnight, then cooled to room temperature. The suspension was dissolved in dichloromethane and loaded onto a plug of silica. The plug was flushed through with ethyl acetate, giving a yellow filtrate. The filtrate was evaporated and purified by flash chromatography (ethyl acetate/hexanes 50:50) to give *2-(3-methoxyphenyl)-4-[(3-methoxyphenyl)amino]-7,8-dihydro-1,6-naphthyridine-5(6H)-thione* (**18**, $R^1 = R^2$ = 3-MeO-Ph) as a yellow solid (34 mg, 0.08 mmol, 57% yield): ^{1}H NMR (200 MHz, $CDCl_3$) δ 3.18 (t, *J* = 6.8 Hz, 2H), 3.61 (td, *J* = 6.8, 3.5 Hz, 2H), 3.82 (s, 3H), 3.85 (s, 3H), 6.78 (dd, *J* = 7.9, 2.3 Hz, 1H), 6.85 (t, *J* = 2.1 Hz, 1H), 6.88 - 7.00 (m, 2H), 7.30 (dd, *J* = 8.0, 2.8 Hz, 1H), 7.34 - 7.44 (m, 3H), 7.48 (dd, *J* = 2.4, 1.4 Hz, 1H), 7.99 (br. s., 1H), 12.09 (s, 1H); MS(ESI) *m*/*z* 392 $[M + H]^+$.

Step 2. Sodium hydride (60% dispersion in oil, 3.5 mg, 0.09 mmol) was suspended in 0.5 mL of dry tetrahydrofuran. A solution of **18** ($R^1 = R^2$ = 3-MeO-Ph, 27 mg, 0.069 mmol) in 0.5 mL of tetrahydrofuran was added drop-wise while stirring. The mixture was stirred at 70 ºC for 30 minutes and was then cooled to room temperature. A solution of methyl iodide (13.5 mg, 0.095 mmol) dissolved in 0.2 mL of dry tetrahydrofuran was added and the mixture was stirred at 70 ºC for 2 hours. The mixture was evaporated and the residue was partitioned between dichloromethane and water. The organic layer was separated, washed with brine and dried over

sodium sulfate. Evaporation gave N-*2-bis(3-methoxyphenyl)-5-(methylthio)-7,8-dihydro-1,6-naphthyridin-4-amine* (**19**, $R^1 = R^2$ = 3-MeO-Ph) as a pale yellow solid (24 mg, 0.056 mmol, 82% yield): ^{1}H NMR (200 MHz, $CDCl_3$) δ 2.43 (s, 3H), 2.79 (t, *J* = 6.8 Hz, 2H), 3.62-3.74 (m, 2H), 3.72 (s, 3H), 3.75 (s, 3H), 6.57 - 6.91 (m, 4H), 7.08 - 7.44 (m, 5H), 7.60 (br. s., 1H); MS(ESI) *m/z* 406 $[M + H]^+$.

Step 3. Compound **19** ($R^1 = R^2$ = 3-MeO-Ph, 12 mg, 0.03 mmol), potassium carbonate (9 mg, 0.06 mmol) and hydroxylamine hydrochloride (4 mg, 0.06 mmol) were suspended in 0.8 mL of ethanol. The mixture was stirred at 70 ºC for 30 min, diisopropylethylamine (0.05 mL, 0.29 mmol) was added and the mixture was stirred at 70 ºC overnight. The solvent was evaporated and the crude was purified by flash chromatography (gradient hexane/ethyl acetate from 50:50 to ethyl acetate) to give **63** as a white solid (3 mg, 0.007 mmol, 23% yield), HPLC purity 91%. ^{1}H NMR (200 MHz, $CDCl_3$) δ 3.16 (br. s., 2H), 3.38 - 3.61 (m, 2H), 3.68 - 3.97 (m, 6H), 5.77 (br. s., 1H), 6.80 - 7.02 (m, 4H), 7.12 - 7.60 (m, 5H), 10.21 (br. s., 1H); MS(ESI) *m/z* 391 $[M + H]^+$.

[(5*Z*)-2-(3-methoxyphenyl)-4-[(3-methoxyphenyl)amino]-7,8-dihydro-1,6-naphthyridin-5(6*H*)-ylidene]cyanamide (64). Compound **19** ($R^1 = R^2$ = 3-MeO-Ph, 12 mg, 0.03 mmol) was treated with cyanamide (5 mg, 0.12 mmol) in 0.8 mL of ethanol. The mixture was stirred at 70 ºC for 45 min, then cooled to room temperature and filtered to give **64** as yellow solid (6 mg, 0.015 mmol, 51% yield), HPLC purity 99%: ^{1}H NMR (200 MHz, $CDCl_3$) δ 3.21 (t, *J* = 6.4 Hz, 2H), 3.73 (td, *J* = 6.5, 2.5 Hz, 2H), 3.84 (s, 3H), 3.85 (s, 3H), 6.70 - 7.02 (m, 4H), 7.27 - 7.42 (m, 5H), 7.43 - 7.50 (m, 1H), 10.57 (br. s., 1H); MS(ESI) *m/z* 400 $[M + H]^+$.

2-(3,4-Difluorophenyl)-4-(quinolin-5-ylamino)-7,8-dihydro-1,6-naphthyridin-5(6*H*)-one (65). Method 1k. White solid, HPLC purity 100%. 39% Yield from **13** (R^1 = 3,4-diF-Ph) and 5-bromoquinoline: ^{1}H NMR (200 MHz, DMSO-d_6) δ 3.06 (t, *J* = 6.6 Hz, 2H), 3.45 - 3.61 (m, 2H), 7.21 (s, 1H), 7.35 - 7.54 (m, 1H), 7.55 - 7.83 (m, 3H), 7.87 (d, *J* = 7.4 Hz, 1H), 7.91 - 8.03 (m, 2H), 8.33 (br. s., 1H), 8.38 (d, *J* = 8.6 Hz, 1H), 8.98 (d, *J* = 3.9 Hz, 1H), 11.65 (s, 1H); MS(ESI) *m*/*z* 403 $[M + H]^+$.

[(5*Z*)-2-(3,4-Difluorophenyl)-4-(quinolin-5-ylamino)-7,8-dihydro-1,6-naphthyridin-5(6*H*)-ylidene]cyanamide (66). Yellow solid, HPLC purity 99%. 26% yield from **19** (R^1 = 3,4-diF-Ph, R^2 = 5-quinolyl, derived from **65** using methods described above): ^{1}H NMR (200 MHz, $CDCl_3$) δ 3.25 (t, *J* = 6.8 Hz, 2H), 3.80 (td, *J* = 6.8, 2.7 Hz, 2H), 6.84 (s, 1H), 7.01 (br. s., 1H), 7.11 (dd, *J* = 18.0, 8.6 Hz, 1H), 7.40 (ddd, *J* = 8.8, 4.0, 2.1 Hz, 1H), 7.48 (dd, *J* = 8.6, 4.3 Hz, 1H), 7.58 (d, *J* = 7.4 Hz, 1H), 7.68 (ddd, *J* = 11.5, 8.0, 2.0 Hz, 1H), 7.82 (t, *J* = 7.8 Hz, 1H), 8.15 (d, *J* = 8.6 Hz, 1H), 8.33 (d, *J* = 8.6 Hz, 1H), 9.01 (dd, *J* = 4.0, 1.5 Hz, 1H), 10.92 (s, 1H); MS(ESI) *m*/*z* 427 $[M + H]^+$.

2-(3'-Hydroxybiphenyl-3-yl)-4-(quinolin-5-ylamino)-7,8-dihydro-1,6-naphthyridin-5(6*H*)-one (67). Method 1k. Yellow solid, HPLC purity 99%. 52% Yield from **16** (R^3 = 3-HO-Ph) and 5-bromoquinoline: ^{1}H NMR (200 MHz, DMSO-d_6) δ 3.08 (t, *J* = 6.4 Hz, 2H), 3.46 - 3.62 (m, 2H), 6.78 (d, *J* = 8.6 Hz, 1H), 6.94 - 7.11 (m, 2H), 7.17 - 7.34 (m, 2H), 7.48 (d, *J* = 7.4 Hz, 1H), 7.56 - 7.68 (m, 1H), 7.67 - 7.91 (m, 3H), 7.91 - 8.01 (m, 1H), 8.07 (s, 1H), 8.31 (br. s., 1H), 8.40 (d, *J* = 8.6 Hz, 1H), 8.99 (d, *J* = 3.9 Hz, 1H), 9.57 (br. s., 1H), 11.63 (s, 1H); MS(ESI) *m*/*z* 459 $[M + H]^+$.

3'-[5-Oxo-4-(quinolin-5-ylamino)-5,6,7,8-tetrahydro-1,6-naphthyridin-2-yl]biphenyl-4-carboxylic acid (68). Method 1k. Pale yellow solid, HPLC purity 97%. 9% Yield from **16** (R^3 = 4-HO_2C-Ph) and 5-bromoquinoline: ^{1}H NMR (200 MHz, DMSO-d_6) δ 3.10 (t, *J* = 6.4 Hz, 2H), 3.54 (br. s., 2H), 7.25 (s, 1H), 7.53 (t, *J* = 7.6 Hz, 1H), 7.63 (dd, *J* = 8.6, 4.3 Hz, 1H), 7.70 - 7.87 (m, 5H), 7.93 (t, *J* = 8.2 Hz, 1H), 8.03 (d, *J* = 8.2 Hz, 2H), 8.17 (s, 1H), 8.35 (br. s., 1H), 8.41 (d, *J* = 8.6 Hz, 1H), 8.99 (d, *J* = 2.7 Hz, 1H), 11.68 (s, 1H), 12.98 (br. s., 1H); MS(ESI) *m*/*z* 487 $[M + H]^+$.

Ethyl 3'-[5-oxo-4-(quinolin-5-ylamino)-5,6,7,8-tetrahydro-1,6-naphthyridin-2-yl]biphenyl-4-carboxylate (69). Method 1k. Brown solid, HPLC purity 91%. 64% Yield from **16** (R^3 = 4-EtO_2C-Ph) and 5-bromoquinoline: ^{1}H NMR (200 MHz, $CDCl_3$) δ 1.41 (t, *J* = 7.0 Hz, 3H), 3.25 (t, *J* = 6.2 Hz, 2H), 3.71 (t, *J* = 6.5 Hz, 2H), 4.40 (q, *J* = 7.0 Hz, 2H), 5.92 (br. s., 1H), 7.03 (s, 1H), 7.37 - 7.54 (m, 2H), 7.55 - 7.73 (m, 3H), 7.63 (d, *J* = 7.8 Hz, 2H), 7.77 (t, *J* = 8.0 Hz, 1H), 7.98 - 8.20 (m, 4H), 8.45 (d, *J* = 8.2 Hz, 1H), 8.98 (d, *J* = 3.1 Hz, 1H), 11.19 (br. s., 1H); MS(ESI) *m*/*z* 515 $[M + H]^+$.

***N*-Cyclopropyl-3'-[5-oxo-4-(quinolin-4-ylamino)-5,6,7,8-tetrahydro-1,6-naphthyridin-2-yl]biphenyl-3-carboxamide (70).** Method 1k. White solid, HPLC purity 96%. 34% Yield from **16** (R^3 = 3-cPrHNOC-Ph) and 4-bromoquinoline: ^{1}H NMR (200 MHz, DMSO-d_6) δ 0.52 - 0.65 (m, 2H), 0.72 (app d, *J* = 6.6 Hz, 2H), 2.75 - 2.98 (m, 1H), 3.14 (t, *J* = 6.2 Hz, 2H), 3.55 (br. s., 2H), 7.47 - 7.93 (m, 8H), 7.98 (s, 1H), 8.01 - 8.22 (m, 4H), 8.34 (br. s., 1H), 8.43 - 8.64 (m, 2H), 8.83 (d, *J* = 5.1 Hz, 1H), 12.44 (s, 1H); MS(ESI) *m*/*z* 526 $[M + H]^+$.

***N*-Cyclopropyl-3'-[4-(isoquinolin-4-ylamino)-5-oxo-5,6,7,8-tetrahydro-1,6-naphthyridin-2-yl]biphenyl-3-carboxamide (71).** Method 1k. White solid, HPLC purity 97%. 42% Yield from

16 (R^3 = 3-cPrNHOC-Ph and 4-bromoisoquinoline: ^{1}H NMR (200 MHz, $CDCl_3$) δ 0.64 (br. s., 2H), 0.90 (app d, *J* = 5.1 Hz, 2H), 2.95 (br. s., 1H), 3.26 (t, *J* = 6.0 Hz, 2H), 3.73 (t, *J* = 6.2 Hz, 2H), 5.90 (br. s., 1H), 6.33 (br. s., 1H), 7.06 (br. s., 1H), 7.37 - 7.58 (m, 3H), 7.60 - 7.90 (m, 5H), 7.93 (br. s., 1H), 8.00 - 8.14 (m, 3H), 8.69 (s, 1H), 9.19 (s, 1H), 11.17 (br. s., 1H); MS(ESI) *m*/*z* 526 $[M + H]^+$.

***N*-Cyclopropyl-3'-[5-oxo-4-(quinolin-5-ylamino)-5,6,7,8-tetrahydro-1,6-naphthyridin-2-yl]biphenyl-3-carboxamide (72).** Method 1k. White solid, HPLC purity 96%. 20% Yield from **16** (R^3 = 3-cPrHNOC-Ph) and 5-bromoquinoline: ^{1}H NMR (200 MHz, DMSO-d_6) δ 0.49 - 0.65 (m, 2H), 0.66 - 0.80 (m, 2H), 2.88 (tt, *J* = 7.0, 3.5 Hz, 1H), 3.09 (t, *J* = 6.6 Hz, 2H), 3.54 (t, *J* = 6.5 Hz, 2H), 7.25 (s, 1H), 7.46 - 7.69 (m, 3H), 7.79 (app d, *J* = 9.4 Hz, 6H), 7.91 - 8.00 (m, 1H), 8.07 (s, 1H), 8.15 (s, 1H), 8.32 (br. s., 1H), 8.41 (d, *J* = 8.2 Hz, 1H), 8.54 (d, *J* = 3.9 Hz, 1H), 8.98 (d, *J* = 2.7 Hz, 1H), 11.66 (s, 1H); MS(ESI) *m*/*z* 526 $[M + H]^+$.

***N*-Cyclopropyl-3'-{4-[(1-oxidoquinolin-5-yl)amino]-5-oxo-5,6,7,8-tetrahydro-1,6-naphthyridin-2-yl}biphenyl-3-carboxamide (73).** Compound **72** (172 mg, 0.28 mmol) was dissolved in 5 mL dichloromethane and cooled to 5 ºC in an ice-bath. meta-Chloroperbenzoic acid (max purity 77%, 142 mg, 0.64 mmol) was added and the mixture was stirred for 30 min at 5 ºC. The mixture was then stirred at room temperature for 2 h. The organics were washed three times with 4% w/v sodium carbonate solution, once with brine and dried over sodium sulfate. The organics were filtered, evaporated and the residue was purified by reverse phase using the SP1 purification system to give 87 as a yellow solid (37 mg, 0.065 mmol, 24% yield), HPLC purity 91%: ^{1}H NMR (200 MHz, DMSO-d_6) δ 0.53 - 0.65 (m, 2H), 0.70 (t, *J* = 3.5 Hz, 2H), 2.78 - 2.96 (m, 1H), 3.10 (t, *J* = 6.6 Hz, 2H), 3.53 (t, *J* = 6.4 Hz, 2H), 7.36 (s, 1H), 7.48 - 7.62 (m,

3H), 7.72 - 7.98 (m, 7H), 8.08 (s, 1H), 8.21 (s, 1H), 8.38 (d, J = 6.6 Hz, 2H), 8.55 (d, J = 3.5 Hz, 1H), 8.66 (d, J = 6.2 Hz, 1H), 11.75 (s, 1H); MS(ESI) m/z 542 $[M + H]^+$.

***N*-[3-(Dimethylamino)propyl]-3'-[5-oxo-4-(quinolin-5-ylamino)-5,6,7,8-tetrahydro-1,6-naphthyridin-2-yl]biphenyl-3-carboxamide (74).** Compound **17** (R^3 = 3-HO_2C-Ph, R^2 = 5-quinolyl, prepared using methods described above, 150 mg, 0.31 mmol) was dissolved in 5 mL of *N*,*N*'-dimethylformamide. 1-Hydroxybenzotriazole hydrate (60 mg, 0.45 mmol) and *N*-(3-dimethylaminopropyl)-*N*′-ethylcarbodiimide hydrochloride (86 mg, 0.45 mmol) were added. The mixture was stirred at room temperature for 30 min. N^1,N^1-dimethylpropane-1,3-diamine (0.077 mL, 0.62 mmol) was added and the mixture was stirred at 50 ºC for 4 h. The solvent was evaporated and 4% potassium carbonate aqueous solution and ethyl acetate were added. The organic layer was separated, washed twice with water and twice with brine, dried with magnesium sulfate, filtered and concentrated. The residue was purified by reverse phase using the SP1 purification system to give **74** as a white solid (28 mg, 0.049 mmol, 16% yield) , HPLC purity 99%: ^{1}H NMR (200 MHz, $CDCl_3$) δ 1.97 (quin, J = 5.8 Hz, 2H), 2.51 (s, 6H), 2.81 (t, J = 6.2 Hz, 2H), 3.24 (t, J = 6.6 Hz, 2H), 3.44 - 3.83 (m, 4H), 6.02 (br. s., 1H), 7.05 (s, 1H), 7.35 - 7.56 (m, 3H), 7.56 - 7.94 (m, 5H), 8.05 (d, J = 8.2 Hz, 1H), 8.14 (d, J = 5.1 Hz, 2H), 8.45 (app d, J = 8.6 Hz, 3H), 8.97 (d, J = 3.1 Hz, 1H), 11.20 (s, 1H); MS(ESI) m/z 571 $[M + H]^+$.

PDE4 activity determination. PDE4 activity from various human recombinant PDE4 subtypes (PDE4B1, PDE4A4, and PDE4D3) was monitored by measuring the hydrolysis of [^{3}H]-cAMP to [^{3}H]-AMP using a PDE-SPA kit from Amersham International as previously described.[40] Enzyme extracts (~4 μg of protein) were incubated in "low binding" plates (Costar 3604) for 60 min at room temperature. The assay mixture (80 μL) containing 15 nM [^{3}H]-cAMP (1 μCi/mL) in the assay buffer (50 mM Tris pH 7.5, 8.3 mM $MgCl_2$, 1.7 mM EGTA) and 10 μL of test

compound. These compounds were re-suspended in DMSO (the final DMSO concentration 5% (v/v)) at a stock concentration of 1 mM. The compounds were tested at different concentrations varying from 10 μM to 10 pM to calculate an IC_{50}. These dilutions were done in 96-well plates. In some cases, plates containing diluted compounds were frozen before being assayed. In these cases, the plates were thawed at room temperature and agitated for 15 min.

Hydrolysis of [^{3}H]-cAMP was initiated by adding 10 μL of a solution containing PDE4 enzyme, and the plate was then incubated under agitation at room temperature. The reaction was stopped after 60 min (with ~10-20% substrate conversion) by addition of 50 μL Phosphodiesterase Scintillation Proximity Assay (SPA) Beads. All reactions were carried out in duplicate. [^{3}H]-AMP, captured by the SPA beads, was determined by counting the plates in a Wallac-Microbeta Trilux scintillation counter 1 h after addition of the beads, although the signal was quite stable, and samples may be counted from 1 to 48 h after bead addition. All experiments were run in duplicates as long as one n was within twice the value of the other (SD $pIC_{50} < 0.2$). Otherwise, further experiments were run until $pIC_{50} < 0.2$. All data reported to two significant figures.

LPS induced TNF-α in human whole blood (HWB-TNF-α). Human whole blood of healthy donors was collected in 50 mL Falcon tubes with heparin (5000 units/mL, Heparin Mayne 5%, MAYNEPHARMA). LPS (lipopolysaccharide from Escherichia coli, Sigma, St. Louis, MO) dissolved in PBS (Dulbecco's phosphate buffered saline, without calcium and magnesium chloride Sigma, St. Louis, MO) was added to the tubes to give a final concentration in the assay of 1 μg/mL and pre-incubated at 37 ºC for 10 min with rocking. Increasing concentrations of different inhibitors (2 μL), dissolved in 100% DMSO, were added to the 96-well plates and 200 μL of blood containing LPS (except for controls) then distributed into wells, plates were shaken

for 1-2 min, sealed with aluminum foil lid (Beckman Coulter), and then incubated for 24 h at 37 ºC under agitation in KelvitronT (Heraeus Instruments).

After 24 h, plates were placed on ice, 50 µL of PBS added, and the reaction was stopped by centrifugation of plates at 2000 rpm (800 G) at 4 ºC for 15 min. Serum obtained was then subjected to ELISA or kept at -80 ºC until use.

TNF-α Determination. The quantification of TNF-α in human serum was performed using commercial ELISA kit (DuoSet) obtained from R&D Systems, Inc., and following the manufacturer's instructions.

Plate Preparation: First, R&D DuoSet ELISA 96-well microplates were coated with 4.0 µg/mL mouse antihuman TNF-R diluted in PBS, overnight at room temperature. After washing, plates were then blocked with PBS containing 1% BSA for a minimum of 1 h at room temperature and then washed.

Assay Procedure: 100 µL of samples or standard was added and incubated at 2 h at room temperature. After washing (ELX406 Select, BIO-TEK), biotinylated anti-hTNF-α antibody was added and incubated at room temperature for 2 h, followed by incubation with streptavidin-peroxidase for 20 min. Detection of bound hTNF-α was carried out with 100 µL of substrate solution (H_2O_2 and tetramethylbenzidine) followed by measurement at 450 nm in a SPECTRA max Plus (Molecular Devices). These experiments were performed 2-3 times using the same experimental design. Duplicates from each series of experiments were averaged and expressed as hTNF-α levels in pg/mL.

Inhibition of LPS-induced neutrophilia in rats. Dry powder administration

A solution of LPS (SIGMA, Ref. L-2630, 100 mg/vial) was prepared in 10 mL PBS (CAMBREX BE17-512F). This was further diluted 1:100 with PBS. Solutions were prepared 24

h before use to ensure dissolution and stored at 4 ºC. Test compounds were micronized before use and co-mixed with lactose to the correct dilution.

Male Sprague-Dawley rats (230-280 g, fasted) were anaesthetized with isofluroane. 5 mg test compound-lactose dry powder mix were loaded into a DP-4 dry powder insufflator fitted with a metal cannula. The cannula was carefully inserted into the trachea of the rats using a laringoscope to guide the needle. Test compound was dispensed with 5 mL air insufflation via a syringe. The cannula was carefully withdrawn and the animals allowed to regain consciousness.

Inhibition of LPS-induced neutrophilia in rats. Microspray administration

A solution of LPS (SIGMA, Ref. L-2630, 100 mg/vial) was prepared in 10 mL PBS (CAMBREX BE17-512F). This was further diluted 1:100 with PBS. Solutions were prepared 24 h before use to ensure dissolution and stored at 4 ºC. Test compounds suspended in PBS containing 0.2% Tween 80 and homogenized in a mortar. Compounds were suspended at their maximum test concentration. Other concentrations were made by 1:10 dilutions with PBS containing 0.2% Tween 80.

Male Sprague-Dawley rats (230-280 g, fasted) were anaesthetized with isoflurane. 0.2 mL test compound suspension were loaded into a Penn-Century microsprayer. The needle was carefully inserted into the trachea of the rats, to about 1 cm from the tracheal carina using a laryngoscope to guide the needle. Test compound was dispensed with rapidly to aerosolize the suspension. The cannula was carefully withdrawn and the animals allowed to regain consciousness.

Nebulization of LPS

1 or 18 h after test compound administration, animals were introduced into perspex chambers and 30 mL LPS solution was aerosolized using the DeVilbiss nebulizer during 40 min. After 4 h, the animals were euthanized with dolethal (2 g/mL, 10 mL/kg i.p). 2 mL PBS was introduced

into the lungs via a cannula and 0.8 mL BAL solution was withdrawn. A further 2 mL PBS was introduced and a further 1.8 mL solution withdrawn Neutrophils were counted directly by flow cytometry using the FACS.

Control groups were formed by i.t. lactose only, i.t. lactose and LPS aerosol and using fluticasone (10% in lactose) and LPS aerosol as positive control.

Animal Studies.

All in vivo experiments were carried out in compliance with the European Committee Directive 2010/63/EU and the Spanish and Catalan laws. Experimental procedures were reviewed by The Animal-Welfare Body of Almirall and approved by the competent authority.

Corresponding Author

Richard S. Roberts, Ph.D.

Rick.s.roberts@gmail.com

tel: +34 699 420 353

Muntaner 545, 08022 Barcelona, Spain

ORCID

0000-0003-2343-6301

Acknowledgments. We acknowledge the significant technical support provided by Silvia Petit, Carmen Cabello, Jordi Serrat, Agustina de la Cal, Dolores Marín, Laura Estrella, Eulàlia Benavent and Lluís Boix. We also acknowledge Montse Soler, Irena Bonin, and Joan Aymami

for the crystal structure determination.. We thank Sonia Espinosa and Josep M. Huerta for their support on physicochemical properties analysis and structural characterization of compounds. This work was funded by Almirall, Spain.

Abbreviations Used. AMP, adenosine monophosphate; Asn, asparagine; BSA, bovine serum albumin; cAMP, cyclic adenosine monophosphate; COPD, chronic obstructive pulmonary disease; cPr, cyclopropyl; DCC, *N*,*N*'-dicyclohexylcarbodiimide; DCM, dichloromethane; DMAP, 4-dimethylaminopyridine; DMF, *N*,*N*-dimethylformamide; DMSO, dimethylsulfoxide; DP, dry powder; EDC, 1-ethyl-3-(3-dimethylaminopropyl)carbodiimide; EGTA, ethylene glycol-bis(β-aminoethyl ether)-*N*,*N*,*N*′,*N*′-tetraacetic acid; ELISA, enzyme-linked immunosorbent assay; FACS, fluorescence-activated cell sorting; Gln, glutamine; GSK, GlaxoSmithKline; HOBt, hydroxybenzotriazole; HWB, human whole blood; i.t., intratracheal; i.v., intravenous; LE, ligand efficiency; LPS, lipopolysaccharide; MS(ESI), mass spectrometry by electrospray ionization; NAP, naphthyridinone; NMR, nuclear magnetic resonance; PAMPA, parallel artificial membrane permeability assay; PBMC, peripheral blood mononucleated cell; PBS, phosphate-buffered saline; PD, pharmacodynamics; PDE, phosphodiesterase; Phe, phenylalanine; PK, pharmacokinetics; Pyr, pyridyl; SAR, structure-activity relation; SPA, scintillation proximity assay; TFA, trifluroacetic acid; THF, tetrahydrofuran; TNFα, tumour necrosis factor alpha; Tris, tris(hydroxymethyl)aminomethane; UCR2, upstream conserved region 2; Val, valine.

Ancilliary Information

Supporting information is available: Table S1. PDE Selectivity Panel for compound **72**, Table S2. Kinase Selectivity Panel for compound **72**, Table S3. Single dose inhibition of LPS-induced lung neutrophilia in rats. Molecular formula strings available.

PBD ID codes: **3**: 3gwt**, 4**: 5k1i, **21**: 5k32. Authors will release the atomic coordinates and experimental data upon article publication.

References

1 Houslay, M. D.; Schafer, P.; Zhang, K. Y. Keynote review: phosphodiesterase-4 as a therapeutic target. *Drug Discov. Today* **2005**, *10*, 1503-1519.

2 Press, N. J.; Banner, K. H. PDE4 inhibitors - a review of the current field. *Prog. Med. Chem*. **2009**, *47*, 37-74.

3 Manning, C. D.; Burman, M.; Christensen, S. B.; Cieslinski, L. B.; Essayan, D. M.; Grous, M.; Torphy, T. J.; Barnette, M. S. Suppression of human inflammatory cell function by subtype-selective PDE4 inhibitors correlates with inhibition of PDE4A and PDE4B. *Br. J. Pharmacol*. **1999**, *128*, 1393-1398.

4 O'Donnell, J. M.; Zhang, H. T. Antidepressant effects of inhibitors of cyclic AMP phosphodiesterase (PDE4). *Trends Pharmacol. Sci*. **2004**, *25*, 158-163.

5 Pagès, L.; Gavaldà, A.; Lehner, M. D. PDE4 inhibitors: a review of current developments (2005 – 2009). *Exp. Opin. Ther. Pat*. **2009**, *19*, 1501-1519.

6 Gavaldà, A.; Roberts. R. S. Phosphodiesterase-4 inhibitors: a review of current developments (2010 - 2012). *Exp. Opin. Ther. Pat.* **2013**, *23*, 997-1016.

7 Martinez, A.; Gil, C. cAMP-specific phosphodiesterase inhibitors: promising drugs for inflammatory and neurological diseases. *Exp. Opin. Ther. Pat*. **2014**, *24*, 1311-1321.

8 Parikh, N.; Chakraborti, A. K. Phosphodiesterase 4 (PDE4) inhibitors in the treatment of COPD: promising drug candidates and future directions. *Curr. Med. Chem*. **2016**, *23*, 129−141.

9 Mulhall, A. M.; Droege, C. A.; Ernst, N. E.; Panos, R. J.; Zafar, M. A. Phosphodiesterase 4 inhibitors for the treatment of chronic obstructive pulmonary disease: a review of current and developing drugs. *Exp. Opin. Invest. Drugs* **2015**, *24*, 1597-1611.

10 (a) Rabe, K. F. Update on roflumilast, a phosphodiesterase 4 inhibitor for the treatment of chronic obstructive pulmonary disease. *Br. J. Pharmacol.* **2011**, *163*, 53–67. (b) Schafer, P. H.; Parton, A.; Gandhi, A. K.; Capone, L.; Adams, M.; Wu, L.; Bartlett, J. B.; Loveland, M. A.; Gilhar, A.; Cheung, Y.-F.; Baillie, G. S.; Houslay, M. D.; Man, H.-W.; Muller, G. W.; Stirling, D. I. Apremilast, a cAMP phosphodiesterase-4 inhibitor,demonstrates anti-inflammatory activity in vitro and in a model of psoriasis. *Br. J. Pharmacol*. **2010**, *159*, 842–855.

11 (a) Jin, S. L.; Conti, M. Induction of the cyclic nucleotide phosphodiesterase PDE4B is essential for LPS-activated TNFα responses. *Proc. Natl. Acad. Sci*. **2002**, *99*, 7628-7633. (b) Manning, C. D.; Burman, M.; Christensen, S. B.; Cieslinski, L. B.; Essayan, D. M.; Grous, M.; Torphy, T. J.; Barnette, M. S. Suppression of human inflammatory cell function by subtype-selective PDE4 inhibitors correlates with inhibition of PDE4A and PDE4B. *Br. J. Pharmacol*. **1999**, *128*, 1393-1398.

12 Lehnart, S. E.; Wehrens, X. H.; Reiken, S.; Warrier, S.; Belevych, A. E.; Harvey, R. D.; Richter, W.; Jin, S. L.; Conti, M.; Marks, A. R. Phosphodiesterase 4D deficiency in the ryanodine-receptor complex promotes heart failure and arrhythmias. *Cell* **2005**, *123*, 25-35.

13 Robichaud, A.; Stamatiou.; P. B.; Jin, S.-L. C.; Lachance, N.; MacDonald, D.; Laliberté, F.; Liu, S.; Huang, Z.; Conti, M.; Chan, C.-C. Deletion of phosphodiesterase 4D in mice shortens a2-adrenoceptor-mediated anaesthesia, a behavioural correlate of emesis. *J. Clin. Invest*. **2002**, *110*, 1045-1052.

14 Xu, R. X.; Hassell, A. M.; Vanderwall, D.; Lambert, M. H.; Holmes, W. D.; Luther, M. A.; Rocque, W. J.; Milburn, M. V.; Zhao, Y.; Ke, H.; Nolte, R. T. Atomic structure of PDE4: insights into phosphodiesterase mechanism and specificity. *Science* **2000**, *288*, 1822-1825.

15 Huai, Q.; Colicelli, J.; Ke, H. The crystal structure of AMP-bound PDE4 suggests a mechanism for phosphodiesterase catalysis. *Biochemistry* **2003**, *42*, 13220-13226.

16 Wang, H.; Robinson, H.; Ke, H. The molecular basis for different recognition of substrates by phosphodiesterase families 4 and 10. *J. Mol. Biol*. **2007**, *371*, 302-307.

17 (a) Wang, H.; Peng, M. S.; Chen, Y.; Geng, J.; Robinson, H.; Houslay, M. D.; Cai, I.; Ke, H. Structures of the four subfamilies of phosphodiesterase-4 provide insight into the selectivity of their inhibitors. *Biochem. J.* **2007**, *408*, 193-201. (b) Fox III, D.; Burgin, A. B.; Gurney, M. E. Structural basis for the design of selective phosphodiesterase. *Cell Signal*. **2014**, *26*, 657–663.

18 Naganuma, K.; Omura, A.; Maekawara, N.; Saitoh, M.; Ohkawa, N.; Kubota, T.; Nagumo, H.; Kodama, T.; Takemura, M.; Ohtsuka, Y.; Nakamura, J.; Tsujita, R.; Kawasaki, K.; Yokoi,

H.; Kawanishi, M. Discovery of selective PDE4B inhibitors. *Bioorg. Med. Chem. Lett*. **2009**, *19*, 3174-3176.

19 For recent examples of inhaled PDE4 inhibitors, see: (a) De Savi, C.; Cox, R. J.; Warner, D. J.; Cook, A. R.; Dickinson, M. R.; McDonough, A.; Morrill, L. C.; Parker, B.; Andrews, G.; Young, S. S.; Gilmour, P. S.; Riley, R.; Dearman, M. S. Efficacious inhaled PDE4 inhibitors with low emetic potential and long duration of action for the treatment of COPD. *J. Med. Chem.* **2014**, *57*, 4661-4676. (b) Kubota, S.; Watanabe, M.; Shirato, M.; Okuno, T.; Higashimoto, I.; Machida, K.; Yokomizo, T.; Inoue, H. An inhaled phosphodiesterase 4 inhibitor E6005 suppresses pulmonary inflammation in mice. *Eur J Pharmacol*. **2015**, *768*, 41-48. (c) Moretto, N.; Caruso, P.; Bosco, R.; Marchini, G.; Pastore, F.; Armani, E.; Amari, G.; Rizzi, A.; Ghidini, E.; De Fanti, R.; Capaldi, C.; Carzaniga, L.; Hirsch, E.; Buccellati, C.; Sala, A.; Carnini, C.; Patacchini, R.; Delcanale, M.; Civelli, M.; Villetti, G.; Facchinetti, F. CHF6001 I: a novel highly potent and selective phosphodiesterase 4 inhibitor with robust anti-inflammatory activity and suitable for topical pulmonary administration. *J Pharmacol. Exp. Ther*. **2015**, *352*, 559-567. (d) Singh, D.; Leaker, B.; Boyce, M.; Nandeuil, M. A.; Collarini, S.; Mariotti, F.; Santoro, D.; Barnes, P. J. A novel inhaled phosphodiesterase 4 inhibitor (CHF6001) reduces the allergen challenge response in asthmatic patients. *Pulm. Pharmacol. Ther*. **2016**, *40*, 1-6.

20 (a) Cooper, A. E.; Ferguson, D.; Grime, D. Optimisation of DMPK by the inhaled route: challenges and approaches. *Curr. Drug Metab*. **2012**, *13*, 457-473. (b) Jones, L. J.; Hughes, A. D. Inhalation by design. *Future Med. Chem*. **2011**, *3*, 1563-1565. (c) Tayab, Z. R.; Hochhaus, G. Pharmacokinetic/pharmacodynamics evaluation of inhalation drugs: application to targeted pulmonary delivery systems. *Exp. Opin. Drug. Deliv*. **2005**, *2*, 519-532.

21 Tolman, J. A.; Williams III, R. O. Advances in the pulmonary delivery of poorly water-soluble drugs: influence of solubilisation on pharmacokinetic properties. *Drug. Dev. Indust. Pharm*. **2010**, *36*, 1-30.

22 Tolman, J. A.; Williams III, R. O. Advances in the pulmonary delivery of poorly water-soluble drugs: influence of solubilisation o pharmacokinetic properties. *Drug Dev. Indust. Pharm.* **2010**, *36*, 1-30.

23 Cooper, A. E.; Ferguson, D.; Grime, K. Optimisation of DMPK by the inhaled route: challenges and approaches. *Curr. Drug Metab*. **2012**, *13*, 457-473.

24 (a) Felding, F.; Sørensen, M. D.; Poulsen, T. D.; Larsen, J.; Andersson, C.; Refer, P.; Engell, K.; Ladefoged, L. G.; Thormann, T.; Vinggaard, A. M.; Hegardt, P.; Søhoel, A.; Nielsen, S. F. Discovery and early clinical development of 2‑{6-[2-(3,5-dichloro-4-pyridyl)acetyl]-2,3-dimethoxyphenoxy}‑N‑propylacetamide (LEO29102), a soft-drug Inhibitor of phosphodiesterase 4 for topical treatment of atopic dermatitis. *J. Med. Chem*. **2014**, *57*, 5893-5903. (b) Bodor, N.; Buchwald, P. Soft drug design: general principles and recent applications. *Med Res Rev*. **2000**, *20*, 58-101.

25 (a) Dahl, G.; Akerud, T. Pharmacokinetics and the drug–target residence time concept. *Drug Discov. Today* **2013**, *18*, 697-707. (b) Vauquelin, G.; Van Liefde, I. Slow antagonist dissociation and long-lasting in vivo receptor protection. *Trends Pharmacol. Sci*. **2006**, *27*, 355-359. (c) Guo, D.; Heitman, L. H.; IJzerman, A. P. The Role of target binding kinetics in drug discovery. *Chem. Med. Chem*. **2015**, *10*, 1793-1796.

26 For some recent reviews on the role of residence time, see: (a) Swinney, D. C. Applications of binding kinetics to drug discovery. *Int. J. Pharm. Med*. **2008**, *22*, 23-34. (b) Swinney, D. C. The role of binding kinetics in therapeutically useful drug action. *Curr. Opin. Drug Discov. Dev*. **2009**, *12*, 31-39. (c) Copeland, R. A. The dynamics of drug-target interactions: drug-target residence time and its impact on efficacy and safety. *Exp. Opin. Drug Discov*. **2010**, *5*, 305-309. (d) Zhang, R.; Monsma, F. Binding kinetics and mechanism of action: toward the discovery and development of better and best in class drugs. *Exp. Opin. Drug Discov*. **2010**, *5*, 1023-1029.

27 (a) Glossop, P. A.; Watson, C. A.; Price, D. A.; Bunnage, M. E.; Middleton, D. S.; Wood, A.; James K.; Roberts, D.; Strang, R. S.; Yeadon, M.; Perros-Huguet, C.; Clarke, N. P.; Trevethick, M. A.; Machin, I.; Stuart, E. F.; Evans, S. M.; Harrison, A. C.; Fairman, D. A.; Agoram. B.; Burrows, J. L.; Feeder, N.; Fulton, C. K.; Dillon, B. R.; Entwistle, D. A.; Spence, F. J. Inhalation by design: novel tertiary amine muscarinic M_3 receptor antagonists with slow off-rate binding kinetics for inhaled once-daily treatment of chronic obstructive pulmonary disease. *J Med Chem*. **2011**, *54*, 6888-6904. (b) Glossop, P. A.; Lane, C. A.; Price, D. A.; Bunnage, M, E.; Lewthwaite, R. A.; James. K.; Brown, A. D.; Yeadon, M.; Perros-Huguet, C.; Trevethick, M. A.; Clarke, N.; P.; Webster, R.; Jones, R. M.; Burrows, J. L.; Feeder, N.; Taylor, S. C.; Spence, F. J. Inhalation by design: novel ultra-long-acting β(2)-adrenoreceptor agonists for inhaled once-daily treatment of asthma and chronic obstructive pulmonary disease that utilize a sulfonamide agonist headgroup. *J. Med. Chem*. **2010**, *53*, 6640-6652.

28 Claus, S.; Weiler, C.; Schiewe, J.; Friess, W. How can we bring high drug doses to the lung? *Eur. J. Pharm. Biopharm*. **2014**, *86*, 1-6.

29 Singh D, Petavy F, Macdonald AJ, et al. The inhaled phosphodiesterase 4 inhibitor GSK256066 reduces allergen challenge responses in asthma. *Respir. Res*. **2010**, *11*, 26-34.

30 Woodrow, M. D.; Ballantine, S. P.; Barker, M. D.; Clarke, B. J.; Dawson, J.; Dean, T. W.; Delves, C. J.; Evans, B.; Gough, S. L.; Guntrip, S. B.; Holman, S.; Holmes, D. S.; Kranz, M.; Lindvaal, M. K.; Lucas, F. S.; Neu, M.; Ranshaw, L. E.; Solanke, Y. E.; Somers, D. O.; Ward, P.; Wiseman, J. O. Quinolines as a novel structural class of potent and selective PDE4 inhibitors. Optimisation for inhaled administration. *Bioorg. Med. Chem. Lett.* **2009**, *19*, 5261-5265.

31 Gràcia, J.; Buil, M. A.; Castro, J.; Eichhorn, P.; Ferrer, M.; Gavaldà, A.; Hernández, B.; Segarra, V.; Lehner, M. D.; Moreno, I.; Pagès, L. Roberts, R. S.; Serrat, J.; Sevilla, S.; Taltavull, J.; Andrés, M.; Cabedo, J.; Vilella, D.; Calama, E.; Carcasona, C.; Miralpeix, M. Biphenyl pyridazinone derivatives as inhaled PDE4 inhibitors: structural biology and structure-activity relationships. *J. Med. Chem*. **2016**, *59*, 10479-10497.

32 Zhang, K. Y.; Card, G. L.; Suzuki, Y.; Artis, D. R.; Fong, D.; Gillette, S.; Hsieh, D.; Neiman, J.; West, B. L.; Zhang, C.; Milburn, M. V.; Kim, S. H.; Schlessinger, J.; Bollag, G. A glutamine switch mechanism for nucleotide selectivity by phosphodiesterases. *Mol. Cell* **2004**, *23*, 279-286. Erratum in: *Mol. Cell* **2004**, *27*, 659.

33 Burgin, A. B.; Magnusson, O. T.; Singh, J.; Witte, P.; Staker, B. L.; Bjornsson, J. M.; Thorsteinsdottir, M.; Hrafnsdottir, S.; Hagen, T.; Kiselyov, A. S.; Stewart, L. J.; Gurney, M. E. Design of phosphodiesterase 4D (PDE4D) allosteric modulators for enhancing cognition with improved safety. *Nat. Biotech*. **2010**, *28*, 63-72.

34 Ferrer, M.; Roberts, R. S.; Sevilla, S. A modular synthesis of novel 4-amino-7,8-dihydro-1,6-naphthyridin-5(6H)-ones as PDE4 inhibitors. *Tetrahedron Lett*. **2013**, *54*, 4821-4825.

35 Hopkins, A. L.; Groom, C. R.; Alex, A. Ligand efficiency: a useful metric for lead selection. *Drug Discov. Today* **2004**, *9*, 430-431.

36 (a) Goto, T.; Shiina, A.; Yoshino, T.; Mizukami, K.; Hirahara, K.; Suzuki, O.; Sogawa, Y.; Takahashi, T.; Mikkaichi, T.; Nakao, N.; Takahashi, M.; Hasegawa, M.; Sasaki, S. Synthesis and biological evaluation of 5-carbamoyl-2-phenylpyrimidine derivatives as novel and potent PDE4 inhibitors. *Bioorg. Med. Chem*. **2013**, *21*, 7025–7037. (b) Goto, T.; Shiina, A.; Yoshino, T.; Mizukami, K.; Hirahara, K.; Suzuki, O.; Sogawa, Y.; Takahashi, T.; Mikkaichi, T.; Nakao, N.; Takahashi, M.; Hasegawa, M.; Sasaki, S. Identification of the fused bicyclic 4-amino-2-phenylpyrimidine derivatives as novel and potent PDE4 inhibitors. *Bioorg. Med. Chem. Lett*. **2013**, *23*, 3325–3328.

37 Le Roux, J.; Leriche, C.; Chamiot-Clerc, P.; Feutrill, J.; Halley, F.; Papin, D.; Derimay, N.; Mugler, C.; Grépin, C.; Schio, L. Preparation and optimization of pyrazolo[1,5-a]pyrimidines as new potent PDE4 inhibitors. *Bioorg. Med. Chem. Lett*. **2016**, *26*, 454-459.

38 Amadasi, A.; Surface, J. A.; Spyrakis, F.; Cozzini, P.; Mozzarelli, A.; Kellogg, G. E. Robust classification of "relevant" water molecules in putative protein binding sites. *J. Med. Chem*. **2008**, *51*, 1063–1067.

39 https://www.drugbank.ca/drugs/DB01656. Accessed on Jan 25, 2018.

40 Percival, M. D.; Yeh, B.; Falgueyret, J. P. Zinc dependent activation of cAMP-specific phosphodiesterase (PDE4A). *Biochem. Biophys. Res. Commun*. **1997**, *241*, 175–180.

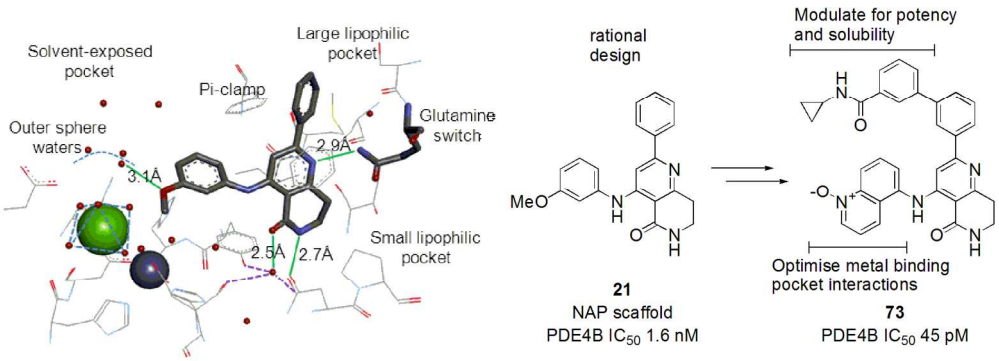

For Table of Contents Use Only

161x58mm (300 x 300 DPI)